Speed in early visual processing

Dissertation

zur Erlangung des akademischen Grades

doctor rerum naturalium
(Dr. rer. nat.)

genehmigt durch die Fakultät für Naturwissenschaften
der Otto-von-Guericke-Universität Magdeburg

von *Dipl.-Psych. Ingo Fründ*
geb. am 28. Februar 1979 in Schweinfurt

Gutachter: Prof. Dr. Christoph S. Herrmann
Prof. Dr. Peter König

eingereicht am: 17. Oktober 2007
verteidigt am: 28. April 2008

Contents

List of Figures

List of Tables

1. Introduction

Imagine yourself in a car driving though a narrow street. Suddenly a blue van shoots out of a side road. In such a situation, it is not important to recognize that the other car is blue, neither that it is a van. The only thing that matters is that you press the break *immediately*.

Now consider the scene in Figure 1.1 on the following page. There are several persons and lots of different objects. The longer we look at this picture, the more details we see. We are able to recognize persons and objects that are partially hidden behind other persons and objects. After some time we will even be able to give a fairly detailed description of the scene without even seeing the picture anymore – we have learned something about the picture.

These two examples impressively demonstrate the great flexibility of the visual system. The very same system rapidly provides a basis for execution of behavioral responses (Kirchner & Thorpe, 2006). At the same time it is up to amazingly detailed representations of the environment and even learning of these representations. In the brain, all these tasks are performed on the basis of action potentials, also called spikes, emitted by densely interconnected neurons. Different investigators have proposed mechanisms how a network of neurons could achieve either the speed (see Thorpe et al., 2001, for review) or the analytic capability (e.g. Freeman, 2003; König & Krüger, 2006; Thielscher & Neumann, 2006) of the visual system. The current report will focus on the impact of motor activity on the visual system. Thus, we will focus our attention in most cases to situations like the one in the first exampe with the blue van. Models aiming to explain such fast behavioral responses, usually consider some sort of interaction between the collective behavior of large groups of neurons and the individual behavior of the single cells constituing the whole group (e.g. Körner et al., 1999; Thorpe et al., 2001; Wyss et al., 2003). Thus, what a single cell does becomes meaningful only in relation to what the whole population does. In the following sections we will review some of the basic ideas of these models. We will first stick to highly simplified discriminations between two alternatives and later proceed to more complex situations.

1.1. Spike timing in neural populations

The patterns of action potentials from single neurons are reasonably well approximated by a poisson process (Dayan & Abbott, 2001, p. 25). This means that

Figure 1.1.: A complex scene with different persons and objects.

(under fixed conditions) for any small time interval there is a fixed probability for the neuron to fire a spike. Thus, the state of the neuron can easily be described by this probability or equivalently by the average rate of spikes that is emitted in a time interval of fixed length. Furthermore, this model allows the response of a neuron to be easily described by changes in this firing rate (Dayan & Abbott, 2001, p. 8 ff).

Figure 1.2 on the next page displays the response of a biologically realistic model neuron (Wilson, 1999, p. 147) to current injection of different strengths. We can immediately see the usefulness of the description by means of the firing rate in this case. The neuron with weak input current ($I = 0.265$nA) emits six spikes, while the neuron with strong input current ($I = 0.270$nA) emits seven spikes. Thus, the information about the strength of the input is contained in the number of action potentials that the cell fired.

What is the first moment at which we can infer the neurons input strength from the neurons firing properties? We do not need to observe the whole time course of the neurons response. In Figure 1.2 it is sufficient to look at the first

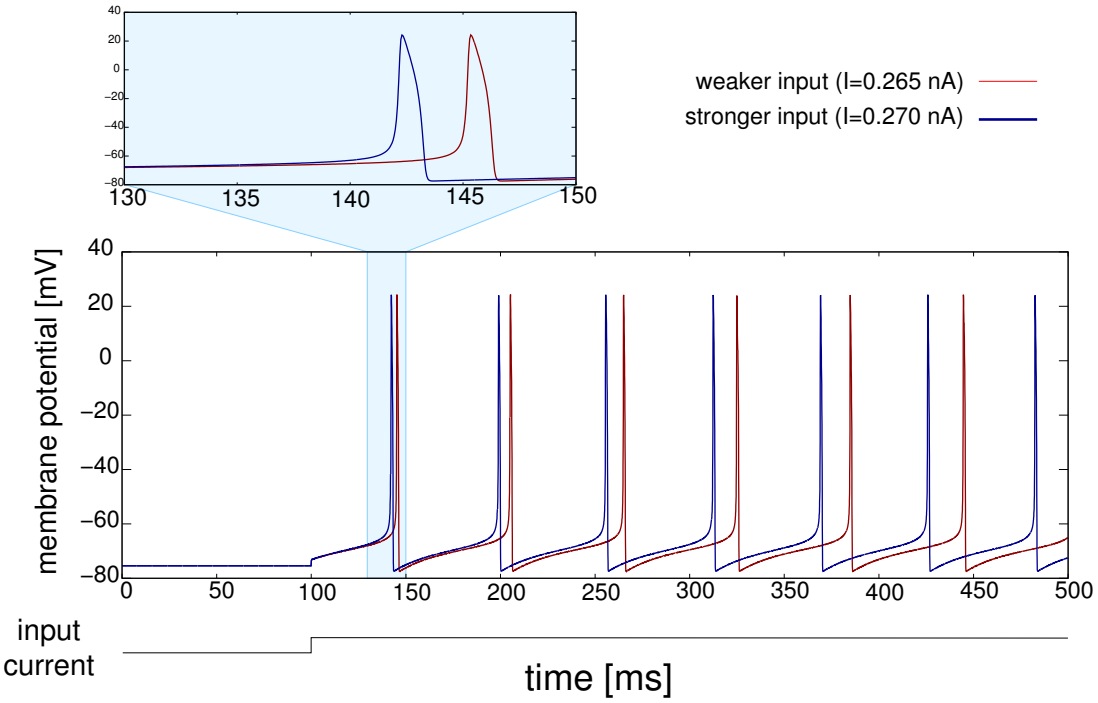

Figure 1.2.:
Two spike trains elicited by current stimulation of different strength. The membrane potential of both model cells is described by the equations $V' = -(17.81 + 47.58V + 33.8V^2)(V - 0.48) - 26R(V + 0.95) + I$, $R' = (-R + 1.29V + 0.79 + 3.3[V + 0.38]^2)/5.6$. The membrane potential $100 \cdot V$ is plotted for $I = 0.265$nA (red) and a slightly stronger input $I = 0.270$nA (blue). The inset at the top of the figure shows an enlarged version of the light blue area in the main figure. Note that different inputs not only result in different firing rates but also in different latency of the first spike.

spike that the neurons fire with the different input currents. With weak input, the neuron fires later than it does with stronger input (also see the inset in Figure 1.2). Thus, the *first* information about the input of the neuron is not contained in the firing rate, but in the timing of the action potentials (Hopfield, 1995). However, this requires the timing of action potentials to be sufficiently reliable. It has been proposed that fast, (shunting) inhibition[1] could ensure the reliability of the temporal firing patterns by integrating information from a larger group of

[1]Shunting inhibition, also called "silent" inhibition, describes the non-linear inhibitory effect of synapses that drive the membrane potential closer to the resting potential (Dayan & Abbott, 2001, p. 160). Synaptic currents associated with shunting inhibition usually have a divisive effect on the target cell (input gain, response to current etc.) and are virtually unnoticed in voltage records (Fregnac et al., 2003).

cells (Fregnac et al., 2003; Körding & König, 2000; Wehr & Zador, 2003). These authors demonstrated that such inhibition sharpens the tuning characteristics of neurons in the visual pathway (Fregnac et al., 2003) and even results in a learning rule that extracts invariant information from dynamic images (Körding & König, 2000; Wyss et al., 2003).

1.2. Oscillations as control signals of neural processing

The situation in 1.2 is particularly simple. There is only one event (a step in the input current) and all we want to learn from the neurons response is the amplitude of this change. Under more natural conditions, e.g. when viewing a complex and probably also moving scene, the input is constantly changing – in time and in space. Thus, it is necessary to (i) constantly reinvestigate the input and (ii) obtain some reference time that enables discrimination of "early" and "late" spikes. From a computational perspective, a solution to both these problems can be obtained by applying an oscillatory modulation to the membrane potential of large groups of neurons in a network (Hopfield, 1995; Körner et al., 1999; Körding & König, 2000; Kupper et al., 2005; Lengyel et al., 2005; Rodemann & Körner, 2003). During a cycle of such an oscillation we can discriminate different phases (c.f. Figure 1.3 on the facing page):

I The neurons are maximally hyperpolarized. There is virtually no chance to evoke an action potential.

II The hyperpolarization decreases and finally changes to a depolarization. At the beginning of this phase only very strong input from many cells can evoke an action potential. Later also weak input from fewer cells can evoke action potentials.

III The neurons are maximally depolarized. Every neuron that could fire an action potential will spike at least in this stage.

IV Those neurons that could spike during the oscillatory cycle are refractory and cannot fire an action potential any more. The network decays to its initial state I.

Thus, the actual processing of the input is now restricted to stage II and the oscillatory signal controls the sequence of the processing stages. It is well known since a long time, that neural tissue tends to oscillate at different frequencies (Başar, 1980; Freeman, 1975). Furthermore, recent data identified neurons that preferred specific phases of local field potential oscillations (Jacobs et al., 2007). Thus, the basic prerequisite of the above mechanism is fullfilled. However, it

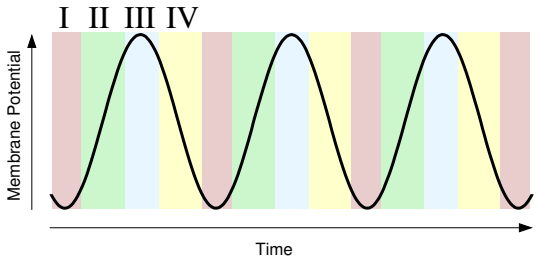

Figure 1.3.:
Phases of an oscillatory cycle. See main text for explanation

should be noted that a large variety of other computational properties can be ascribed to oscillatory brain signals too (e.g. Lengyel et al., 2005).

Using an oscillatory control signal has successfully been employed to temporally encode information about a stimulus in neural firing patterns (Rodemann & Körner, 2003) and to integrate feedforward and feedback processing (Rodemann & Körner, 2001). However, a static oscillatory signal will fail if the input (e.g. from the retina) is changing. VanRullen & Koch (2003) argue that instead oscillatory signals in the brain should adapt to the requirements of the current task. Indeed, Kupper et al. (2005) were able to reconstruct input images from spike timings controlled by an oscillatory signal only, if the oscillatory signal was reset to a fixed phase every time a reasonably large change in the input image appeared. It has been proposed that directly after a stimulus has been presented, the oscillatory control signal should be actively reset, while at later times it would be sufficient to keep the oscillatory signal synchronized amoung those neurons that contain information that might be integrated into the percept (Körner et al., 1999). The reset mechanism should lead to a more or less constant relationship of the phase of the oscillatory signal to the onset of a stimulus after multiple stimulus representations. In contrast, keeping the oscillation synchronized accross a suffient group of neurons should be expressed in a more or less constant phase of the oscillatory control signal in these neurons but not necessarily a constant phase accross stimulus presentations.

1.3. Measuring large scale brain oscillations

A common method to measure synchronous activity from large numbers of neurons is the electroencephalogram (EEG Berger, 1929, see also Section 2.1). By means of a strong amplifier, electrical signals are recorded from electrodes affixed to the scalp of a person (or an animal). These signals can be associated with summed postsynaptic potentials of $\approx 60 \times 10^6$ neurons (Nunez & Srinivasan, 2006). If these potentials are synchronized, the potential can be measured on the scalp. Thus, the EEG seems to be the method of choice to investigate the large scale control signals described in section 1.2. Indeed, EEG oscillations are known since the very first days of the EEG (Berger, 1929). Different investigators have argued that stimulus induced reorganization/resetting of these spon-

taneously emerging oscillations might constitute the basis of the event related potential observed after sensory stimulation (Başar, 1980; Makeig et al., 2002; Wright et al., 1990).

Two fundamental types of oscillatory EEG responses have been identified (see Basar-Eroglu et al., 1996; Tallon-Baudry & Bertrand, 1999, for review). These two types of responses are illustrated in Figure 1.4 on the next page in part (A). The top three rows of this Figure display possible single trial responses in blue. Between 50 and 100ms, an oscillatory response peaks in every trial. This response has the same time course in all trials. Such a response is usually called *evoked*. It can be observed in a simple pointwise average across all single trials as demonstrated for 200 trials in the forth row of Figure 1.4 (A, marked in green). Figure 1.4 (A) also displays another type of response. This is a second oscillatory burst, peaking between 450 and 550ms. However, this second type of response jitters in latency with respect to stimulus onset (assumed to be at 0ms). As a consequence, this second type of response is virtually absent in the average across single trials in the forth row (time range marked in yellow). To quantify such *induced* responses, it is now common to average single trial power or amplitude (e.g. Gruber & Müller, 2005; Jensen et al., 2002; Lachaux et al., 2005; Tallon-Baudry et al., 1996b). In Figure 1.4 (A) time courses of instantaneous amplitude (so called envelopes) are plotted in red. An average across 200 of these envelopes is plotted in the bottom row of Figure 1.4. In contrast to the simple average in the forth row, the induced response is now clearly visible in the average of the envelopes. This model is of course a very coarse simplification. The brain is probably not quiet between the oscillatory responses. Furthermore, a prototypical response as suggested by Figure 1.4 (A) seems rather unrealistic.

In Figure 1.4 (B) the responses of an oscillating linear system to stochastic inputs are shown. The system is constantly stimulated by gaussian white noise with an amplitude of $\sigma = 1$. There are two exceptions to this rule. (i) At $t = 0$s, the input is set to a fixed value of 2. (ii) In the time range from $t = 0.4$s to $t = 0.5$s the amplitude of the input noise first rises until it reaches a value of 2 at $t = 0.45$s. From $t = 0.45$s to $t = 0.5$s, the amplitude of the input noise falls back to 1. In the single realizations (top three panels in Figure 1.4), neither responses to the fixed input (i) nor to the input amplitude change (ii) can be discerned from the random variations due to the noisy input. However, averaging the signals (fourth row in Figure 1.4, labeled "average") reveals a clear response to the fixed input (i) but virtually no response to the gradual change of the input signal (ii). In contrast, if we average the envelopes of the single realizations of the output signal (blue curves in Figure 1.4), the situation reverses. The average envelope increases in response to increased input amplitude (ii), while there is virtully no response to the fixed input. The inputs to our simplified model may be associated with two different types of input than can be imposed on neural tissue. Input from the thalamus to the cortex begins with a transient pulse (Funke & Wörgötter, 1997). The fixed input (i) to our linear oscillating system might be a reduced model for

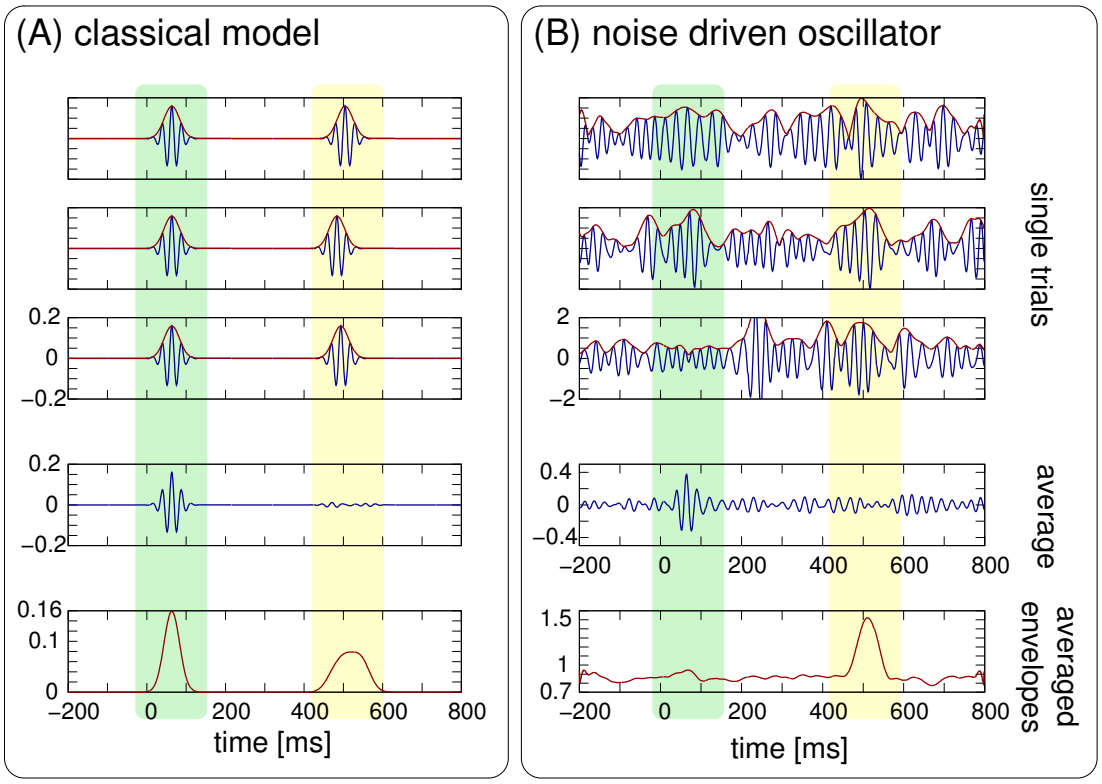

Figure 1.4.:
Poststimulus EEG dynamics and possible underlying machanisms. (A) The classical model with an evoked response (green underlay) and an induced response (yellow underlay). This model assumes a prototypical response (here modeled as a modulated gaussian $1/(2\pi)\cos(2\pi 40[t-64-t_0])\exp(-[t-64-t_0]^2/[2\sigma^2])$, $\sigma = 20$ms). If the onset t_0 of this response is constant over time, this results in an evoked response. If the onset of this response jitters across trials this results in an induced response (modified after Tallon-Baudry & Bertrand, 1999). The top three rows show single trial responses, the bottom rows show an average across 200 single trials (blue lines) and an average across the 200 single trial envelopes (dark red lines). (B) Different inputs to a stochastically driven linear oscillator. The top three rows of the image show time courses of the output of a linear oscillator (impulse response as in (A), displayed in blue) and envelopes of the output (displayed in red). The oscillator was stimulated with gaussian white noise with time varying standard deviation ($\mu = 0$, $\sigma(t) = 1.5 - \cos(2\pi(t - 0.45\text{s})/0.1\text{s})$ if $0.4\text{s} \leq t \leq 0.5\text{s}$ and $\sigma(t) = 1$ otherwise) except for $t = 0$s. At $t = 0$ the input to the oscillator was set to the constant value 2. In the fourth row (average) the average time course of the oscillators output signal from 200 realizations of the input signal is shown. In the bottom row (averaged envelopes) the average of the envelope signals is shown. Observe, that the direct average detects the response of the fixed input, while the average of the envelopes detects the output to increased input standard deviation.

this kind of input. The membrane potentials of neocortical neurons *in vivo* are fluctuating with an approximately gaussian distribution (Destexhe et al., 2003). We believe that input of type (ii) might model the effects of increased neural firing in a sufficiently large group of cells. Although EEG signals do not seem to be generated by a linear system (Basar, 1990; Moss et al., 2004; Stam, 2005; Sarbadhikari & Chakrabarty, 2001), linearity seems to be a valid approximation at least on a short time scale (Freeman, 1975; Wright et al., 1990). As mentioned above, the two types of responses can indeed be observed in scalp measured EEG signals, although in these cases their origin is less clear than in our model. We can thus generalize our notion of evoked and induced responses. Oscillatory responses that are detectable in a simple average of the ongoing EEG (with respect to a repeated stimulation) are called *evoked* responses, while responses that are only detectable in averages of envelopes are termed *induced* responses (Basar-Eroglu et al., 1996; Tallon-Baudry & Bertrand, 1999). These two response types are often charaterized as being phase-locked to a stimulus (evoked) or not phase-locked (induced).

In the simulation in Figure 1.4 on the preceding page, we have used a linear system with a fairly narrow frequency response. Typical scalp measured responses are characterized by far more different frequencies. In these cases, a clear oscillatory structure is not always obvious. However, it has been argued that the scalp measured EEG signals represent the superimposed activity of different oscillatory systems working in parallel (Başar, 1980; VanRullen & Koch, 2003). Başar (1980) proposes that these subsystems could be differentiated as distinct peaks in the power spectrum of the EEG. Most of these oscillatory systems can also be dissociated by their functional characteristics. For instance rhythmic activity between 8 and 13Hz over the motor cortex is selectively abolished before movements (see Pineda, 2005, for review). A similar decrease can be observed for 8 to 13Hz (α) activity over posterior areas after visual stimulation (Klimesch, 1999). Other frequency ranges exhibit specific changes during short term memory tasks (Klimesch, 1999; Klimesch et al., 2006, θ, 5-7Hz) or gestalt perception (Tallon-Baudry et al., 1996a, γ, 30-90Hz). VanRullen & Koch (2003) state that different frequencies seem to be employed for different tasks. They particularly argue that frequencies around 40 Hz should play a role in generating speeded responses, as this frequency is present in both, reaction time histograms and brain signals. With respect to reaction time histograms, Vorberg & Schwarz (1987) note, that "'histograms from unimodal populations are quite likely to exhibit multiple peaks unless extremely large sample sizes are used."' Extremely large in their case means of the order of 10^5-10^6. As normal behavioral experiments usualy do not employ such large sample sizes, Jokeit (1990) suggested to consider pairwise differences between reaction times. If there was indeed a periodicity in the true reaction time distribution, this would persist in the histogram of pairwise reaction time differences. In contrast, a spurious periodicity that was due to an insufficiently large sample would clearly be diminished in that case. In

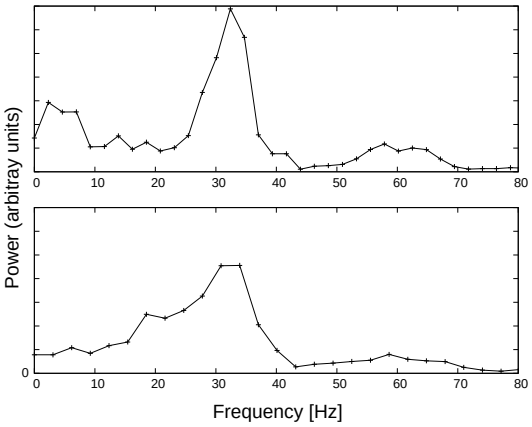

Figure 1.5.:
Power spectra of reaction time difference histograms from two different participants

Figure 1.5, we present power spectra computed from the histograms of reaction time differences from two participants performing speeded button presses. Supporting the claim by VanRullen & Koch (2003) a prominent peak between 30 and 40 Hz can be observed in both panels. These results suggest an important role for γ (30-90 Hz) oscillations in the context of visual processing in relation to rapid motor acts. In the following, we will briefly review previous findings on oscillatory brain activity in the γ frequency range.

1.4. Previous findings on γ oscillations: matching and utilization

In the previous section, we suggested that oscillatory brain activity in the γ frequency range could play a role for rapid perception. Indeed, modulations of γ activity are often found in response to visual stimulation (e.g. Busch et al., 2004; Herrmann et al., 1999; Hoogenboom et al., 2006; Keil et al., 2001; Tallon-Baudry et al., 1996b) and auditory stimulation (Debener et al., 2003; Jokeit & Makeig, 1994; Kaiser & Lutzenberger, 2005; Tiitinen et al., 1993). The distinction between evoked and induced responses from section 1.3 applies well to γ band activity. Evoked and induced γ band responses usually show no temporal overlap: early responses occur around 90 ms (after auditory stimulation earlier) and can be characterized as evoked responses, while later responses are usually induced in the sense of section 1.3 (Herrmann et al., 2004; Tallon-Baudry & Bertrand, 1999).

Evoked γ band responses (eGBRs) display a strong dependence on physical factors of the stimulus (Busch et al., 2004; Fründ et al., 2007; Herrmann & Mecklinger, 2000). For instance, large, centrally presented stimuli evoke significantly stonger eGBRs than smaller versions or more peripherally presented versions of the same stimuli (Busch et al., 2004). Not only stimulus factors influence eGBRs. In particular attention seems to facilitate eGBRs (Busch et al., 2006; Debener

et al., 2003; Herrmann et al., 1999; Tiitinen et al., 1993). Recently it has also been demonstrated, that eGBRs are enhanced in response to line drawings of familiar objects compared to random arrangements of the same lines (Herrmann et al., 2004).

Induced γ band responses (iGBRs) on the other hand, arise relatively independent of stimulus factors after stimulation with semantically meaningful pictures (Busch et al., 2006; Gruber & Müller, 2005). It has been suggested, that iGBRs would be related to the maintenance of object representations (Gruber & Müller, 2006; Tallon-Baudry & Bertrand, 1999), because they are also visible during the retention interval of a short term memory task (Tallon-Baudry et al., 1998) and emerge when participants detect figures hidden in noise (Tallon-Baudry et al., 1997). Further evidence supporting this hypothesis comes from Gruber & Müller (2005). These authors observed, that iGBRs increased for repeated presentations of initially unknown pictures. Based on intracranial recordings from animals, Singer & Gray (1995) suggested, that γ band synchrony of cells in different brain areas could serve as a "tag" indicating that these cells belong to the same object representation. Furthermore, it has been shown, that such synchrony also facilitates the allocation of attention (Fries et al., 2001). Studies measuring long range synchrony of γ oscillations from the scalp of healthy humans support this view (Gruber & Müller, 2005; Rodriguez et al., 1999).

There have been only few attempts to integrate the findings about evoked and induced γ band oscillations in a common theoretical framework. Körner et al. (1999) suggested a neural architecture in which spike latency based feedforward processing of spike timings is refined by feedback activity based on an internal representation of the environment. In their model, γ oscillations serve as a common temporal reference for feedforward and feedback activity (similar to Section 1.2). They demonstrate, that resetting the phase of the ongoing γ oscillations sharpens the representations after sudden changes of the stimulus (Kupper et al., 2005). Without such a phase-reset, these authors observed increasingly scattered responses, that could not form a reliable basis for a latency code. In recordings of electrical activity averaged from many neurons, such a reset could manifest in an evoked γ band response. More recently, it has been suggested that matching of incoming information with stored long term memory representations should enhance evoked γ responses, while subsequent utilization of the outcome of this matching process should enhance induced γ responses (Herrmann et al., 2004).

In addition to the above findings about the perceptual role of γ oscillations, some reports describe relations between reaction time and γ oscillations. Jokeit & Makeig (1994) report that fast reacting participants displayed a stronger enhancement of γ power than slow reacting participants, when reacting to auditory stimulation. Also the latency of stimulus related γ power enhancements correlates with reaction time (Haig et al., 1999). This is in line with the observation, that γ oscillations are facilitated if participants have to perform a motor response at all (De Pascalis & Ray, 1998). These studies investigated γ power, which is equiva-

lent to analyzing the envelopes, i.e. induced γ responses as in Figure 1.4 on page 7. However, from the computational perspective outlined in section 1.2 on page 4, a relation between evoked (phase locked to the stimulus) γ responses and reaction time would seem particularly plausible. There is only indirect evidence regarding this topic. In studies investigating eGBRs in schizophrenic patients, decreased phase-locking of γ band responses is accompanied by prolongated reaction times in patients compared to healthy controls (Spencer et al., 2003).

2. General Methods

In this chapter we will give a brief overview of the methods used throughout the following experiments. These include the general EEG recording setup, which will be described in section 2.1. In section 2.2 on page 17 ff, we will define some standard methods to quantify the event related oscillatory dynamics of the EEG. This will include a more quantitative definition of the concepts of evoked and induced responses from section 1.3 on page 5.

2.1. Electroencephalographic measurements

2.1.1. Generation of the electroencephalographic signal

As briefly mentioned in section 1.3 on page 5, the electroencephalogram (EEG) is a method for measuring summed postsynaptic potentials from large groups of neurons (Berger, 1929; Nunez & Srinivasan, 2006). The synapses that connect neurons usually have a rather local effect. If a synapse becomes active, this results in a change of the permeability of the postsynaptic cell membrane to different types of ions. These ions carry charge through the cell membrane which results in a small current through the cell membrane. These local currents through the cell membrane generate electrical sources or sinks depending on whether the currents have a hyperpolarizing or depolarizing effect on the cells membrane potential. If all this happens at one end of a lengthy neuron, for example the apical dendrite of a cortical pyramidal cell, this neuron for a short moment behaves like an electrical dipole. Such a dipole has a characteristic electrical field. A sketch of such an electrical field is illustrated in Figure 2.1 on the next page (A).

Under normal conditions, there will usually be lots of such electrical dipoles in cortical tissue[1]. Whether or not the extracellular currents associated with postsynaptic potentials can be measured on the scalp is highly dependent on the geometrical arrangement of these cells. In Figure 2.1 (B) and (C) the summed electric fields of 30 dipoles that were randomly positioned in a restricted area (marked by the dotted box) are shown as iso lines. In display (B) all the dipoles have the same orientation (i.e. same direction of potential gradient) while the

[1]Note that cells that do not have such a lengthy morphology as the one scematically drawn in Figure 2.1 (A) will not have such a prototypical electric field. In many cases their extracellular currents will even average to zero. This is particularly the case for most subcortical structures.

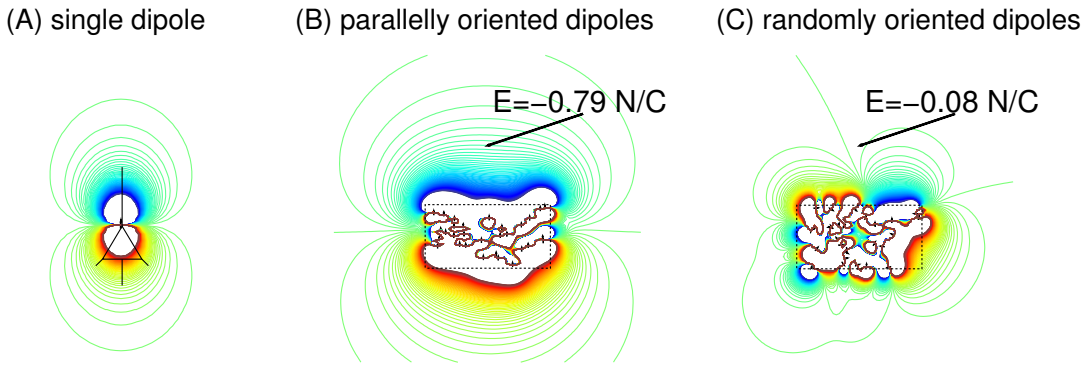

Figure 2.1.:
Electric dipole fields. (A) Iso lines of the electric field of a single dipole. Black lines indicate the possible position of a cortical pyramidal cell. (B) Iso lines of the electric field of 30 randomly positioned, iso-oriented dipoles. The area in which the dipoles have been positioned is marked by a dashed box. (C) like (B) but dipole orientations are random. Iso lines are colored according field strength – blue iso lines correspond to negative field strength, red iso lines to positive field strength. Note that electrical field strength differs by a factor of nearly 10 at the position marked in parts (B) and (C).

orientations in display (C) have been drawn from a random distribution. The strength of the electric field at the same position (with respect to the dipole area) is nearly 10 times larger in Figure 2.1 (B) than in Figure 2.1 (C). In cortical tissue, however, pyramidal cells are usually iso-oriented, perpendicular to the cortical surface. However, there are some exceptions to this rule. Close to the ground of a sulcus for instance, there are dipoles with virtually all possible orientation. In such a constellation, it will not be possible to measure an EEG signal from a distance (e.g. from the scalp). Thus, we conclude that the EEG mainly measures *postsynaptic* potentials from *apical dendrites* of pyramidal cells in *cortical* tissue.

In contrast to most other methods that record electric activity from the brain, the EEG usually measures the activity from outside the brain – from the scalp. In order to be measured from the scalp, these signals have to cross several layers of tissue and in particular the skull, which leads to significant smearing and attenuation of the signals (Nunez & Srinivasan, 2006). This requires a sufficiently strong amplifier. Unfortunately such an amplifier will also amplify signals that are not related to brain activity, such as 50Hz line activity, radio waves, muscle activity or eye movements. In the experiments described in this report, the EEG was recorded using a BrainAmp amplifier (Brain Products, Munich).

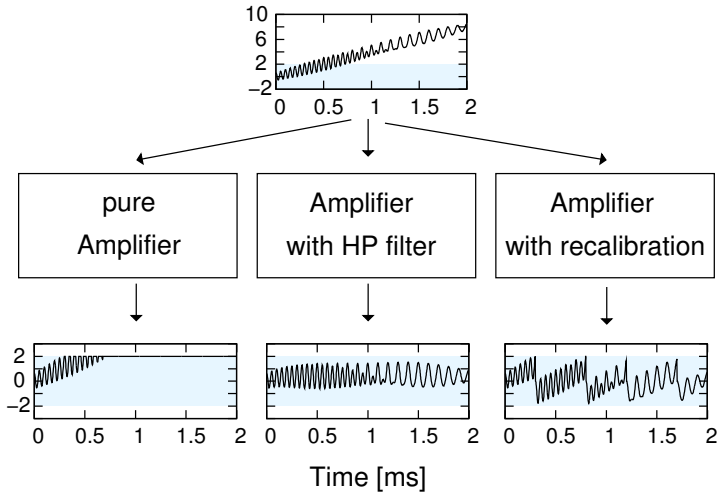

Figure 2.2.:
Strategies to avoid amplifier saturation. at the top of the figure, an artificial signal is shown. The output of a simulated amplifier is displayed at the bottom of the figure. The amplifier range (indicated in light blue) of this simulated amplifier ranges from -2 to 2 (in arbirary units). Left panel, bottom: no mechanism to avoid amplifier saturation. Middle panel, bottom: a high pass filter is applied to avoid amplifier saturation. Right panel, bottom: the signal is reset from time to time. Note that, high pass filtering does not disrupt the signal, but destroys the slow drift, while resetting disrupts the signal but conserves the slow drift in the signal.

2.1.2. Reducing environmental noise

A serious problem for electroencephalographic measurements are artifacts from electrical activity that is not related to the brain. To reduce influences from electric fields associated with line activity or radio waves, participants sat in an electrically shielded and sound attenuated room (iac, niederkrüchten, germany) during the experiments. The stimulation monitor was placed outside this recording cabin behind an electrically shielded window. All devices inside the cabin were battery operated to avoid line frequency interference. Cables connecting devices in the interior of the cabin to devices outside the cabin can transfer electric activity into the cabin, thus undoing the shielding effect of the cabin. Therefore, EEG data were digitized inside the cabin (at a rate of 500Hz) and transferred to a computer outside the cabin by means of a fiber optic cable.

In electroencephalographic recordings, the signal sometimes shows slow drifts of high amplitude over extended time intervals. This poses problems for the amplifier, which has a limited amplification range. At the borders of this range the

amplifier saturates and a further increase of the input signal (i.e. EEG) does not lead to a further increase of the amplifier output signal (i.e. the *recorded* EEG). This is illustrated for an artificial signal in left part of figure 2.2 on the preceding page. To avoid such saturation effects different strategies can be applied. the simplest version is to apply an analog high pass filter before the signal is amplified. As illustrated in the middle part of figure 2.2, such a filter will reduce any slow changes of the input signal. This is particularly relevant, if such slow changes contain relevant parts of the signal. In such a case the alternative solution is, to recalibrate the amplifier every time it approaches saturation. This case is shown in the right part of figure 2.2. We will use different strategies to avoid amplifier saturation in the different experiments.

2.1.3. Physiological artifacts

As mentioned on page 14, there are also artifacts, that can be associated with physiological processes. For instance, eye movements generate characteristic, step like potential changes in the EEG. Similarly, activity from muscles close to the scalp generates potential bursts with a broad band frequency spectrum. These bursts contain a significant amount of energy in the frequency range between 30 and 80 Hz and could therefore easily be mistaken for EEG γ oscillations (Herrmann et al., 2005). Although these, and other physiological artifacts, may be related to an experimental condition, they can obscure the EEG signals. If a good model, describing the influence of an artifact source is available, one can try to apply an algorithm to correct for these artifacts (see Talsma & Woldorff, 2005, for an overview). For the experiments presented in the current report, we employed another approach. Data segments that contained artifacts were completely excluded from subsequent analysis. This way some parts of the signal, that actually contained meaningful information might have been discarded, too. However, this procedure ensured that only artifact free data were included into the analysis.

2.1.4. The problem of electrode placements

From the fact, that EEG represents summed activity from very large numbers of neurons, it might be inferred that electrode placement is not important for measuring EEG. this is only partly true. Due to the bipolar structure of electric fields of the EEG (Nunez & Srinivasan, 2006), interpretation and comparison of EEG data is only possible if the exact measurement positions are known. Jasper (1958) presented a system to standardize positions of 19 electrodes on the scalp. He divided the distance between nasion and inion into segments of 10%, 20%, 20%, 20%, 20%, and 10% to obtain five positions along the sagittal axis of the head. Lateral positions are integer multiples of the 20% nasion-inion distance from this central line to the left or right respectively. Jasper's nomenclature

roughly labels the sagittal positions by the letters F, C, P, O for frontal, central, parietal and occipital[2]. Odd numbers refer to electrodes in the left hemisphere, even numbers refer to electrodes in the right hemisphere. More lateral positions are marked by larger numbers. Electrodes on the midline are labeled with a "z".

Modern EEG systems can measure EEG from a lot more than 19 electrodes. For instance the company Geodesics Inc. offers EEG systems with 256 electrodes (http://www.egi.com/, offer from 5. March 2007). The positions of such large numbers of electrodes can hardly be described by Jaspers' 10-20 system. Therefore, extensions of this system have been proposed to include larger numbers of electrodes (e.g. Chatrian et al., 1985). In the experiments in Chapters 3, 4, and 5 such an extended version of the original 10-20 sytem is used to label electrode locations. This way electrode labels roughly correspond to the cortical lobe below them[3].

2.2. Time-frequency analysis

2.2.1. Classical EEG analysis and its drawbacks

The classical method to analyze the EEG consists of computing the average event related potential (ERP). This is a pointwise average of many trials from the same experimental condition. Although this method has proven very useful and is now one of the standard methods for analyzing the EEG, information about oscillatory components of the EEG is less obvious from the ERP waveforms. Information about oscillatory components on the contrary is contained in the power spectral density (e.g. Başar, 1980). The power spectral density is the fourier transform of the autocorrelation function and describes frequency and strength of periodicities in a signal sampled from a linear stationary stochastic process[4]. Unfortunately, the EEG is generally agreed to be neither stationary and nor linear (e.g. Rosso et al., 2001). At some point, oscillations arise, at another point slow changes in the signal emerge or sudden singular spikes can be observed. A common strategy to overcome this problem is, to analyze only small segments of the signal. This strategy will simultaneously represent the signal in time (of the segment) and frequency (within the segment). We will first consider the general approach of

[2] In addition to this rule, the letters T for temporal and Fp for fronto-polar are used.

[3] Due to the dipolar structure of fields measured by the EEG, this does not necessarily imply that activity measured by these electrodes originates from that lobe (Nunez & Srinivasan, 2006).

[4] A stochastic process is a sequence of random variables $(X_i)_i$. In general, there are no restriction about the interrelations of the X_i, or their distributions. Stationarity characterizes a stochstic process for which the distributions of all X_i are the same. Linearity requires that the interrelations between the X_i are linear. All information about a linear, stationary stochastic process is contained in its autocorrelation function, or equivalently its power spectrum (Oppenheim et al., 2004).

time frequency analyses and then proceed to the wavelet transform, which is used in this report. Finally we will derive three statistical quantities, that can be used to characterize EEG signals in time and frequency.

2.2.2. The general notion of time-frequency analysis

The basic idea of time-frequency analysis of a signal $x(t)$ is to compute a representation of the form

$$Lx(t,f) = \int x(\tau)\overline{\phi(t-\tau;f)}\,\mathrm{d}\tau = (x * \phi(\,\cdot\,;f))(t), \tag{2.1}$$

where $\phi(t;f)$ is a function with a suitable localization in time as well as frequency (Louis et al., 1998). The parameter f can tune ϕ to different peak frequencies. The $*$ operator denotes (complex) convolution and overlining indicates complex conjugation. For fixed f we can see, that $Lx(t,f)$ is just the convolution of x and $\phi(\,\cdot\,;f)$. As $\phi(\,\cdot\,;f)$ is limited to a finite frequency band, the operator L will act like a (complex) band pass filter. This implies, that the most general time-frequency representation of a signal $x(t)$ can be obtained by applying a set of band pass filters to the signal. However, setting the band limits of such filters will generally be a somewhat arbitrary choice. Başar (1980) suggested to adapt the band limits of the filters in accordance with the frequency characteristic of the ERP. This approach will not be able to track transient changes in response frequency. Despite this shortcoming, virtually all time-frequency analyses are at the heart a (possibly infinite) set of filters (Louis et al., 1998; Oppenheim et al., 2004).

If we set $\phi(t;f) = (1/\sqrt{2\pi})w(t)\exp(-2\pi\imath ft)$ with a fixed, real valued window function $w(t)$ in equation (2.1), we obtain the *windowed fourier transform*. An overview of different windows can be found in most books about signal processing (e.g. Oppenheim et al., 2004). Inserting this definition of ϕ into equation (2.1) and denoting the fourier transform operator as F yields

$$\begin{aligned}
Lx(t,f) &= \int x(\tau)w(t-\tau)\exp(2\pi\imath f(t-\tau))\,\mathrm{d}\tau && (2.2)\\
&= \int x(\tau)w(t-\tau)\exp(2\pi\imath ft)\exp(-2\pi\imath f\tau)\,\mathrm{d}\tau && (2.3)\\
&= \exp(2\pi\imath ft)\Big(\int (x(\tau)w(t-\tau)\exp(-2\pi\imath f\tau)\,\mathrm{d}\tau\Big) && (2.4)\\
&= \exp(2\pi\imath ft)F\big((xw(t-\,\cdot\,))(f)\big) && (2.5)\\
&= \exp(2\pi\imath ft)(Fx * Fw(t-\,\cdot\,))(f). && (2.6)
\end{aligned}$$

In (2.5) we used the parseval theorem. As can be seen from (2.6), the fourier transform of x around time t is smeared due to the convolution with the fourier

transform of the window. At the same time, the signal x is smeared in time due to the convolution with the window in (2.2).

Equations (2.2) to (2.6) indicate a fundamental problem of time-frequency analyses: Time and frequency of an event can not be represented with infinite precision at the same time. The Heisenberg uncertainty principle states that the product of the variances in time and frequency has a lower bound (Louis et al., 1998). Time-frequency analysis therefore always represents a compromise between temporal resolution and frequency resolution. For the windowed fourier transform, this compromise is always the same. It only depends on the window function $w(t)$. Also see Figure 2.3.

2.2.3. The wavelet transform

Generally, we can expect high frequency components to vary fast and low frequency components to vary slow. The *wavelet transform* accounts for this, by varying frequency and window width at the same time. This is done by introducing a scaling operator

$$S_a\phi(t) = a^{-1/2}\phi\Big(\frac{t}{a}\Big), \quad a > 0.$$

Due to the scaling property of the fourier transform, we see that

$$F\big(S_a\phi(\,\cdot\,)\big)(f) = F\Big(a^{-1/2}\phi\big(\frac{\cdot}{a}\big)\Big)(f) = a^{-1/2}F\Big(\phi\big(\frac{\cdot}{a}\big)\Big)(f) = a^{1/2}(F\phi)(af).$$

For high values of a, the function $S_a\phi$ becomes very broad in time but very concentrated in frequency at relatively low frequencies. For low values of a, the function $S_a\phi$ becomes concentrated in time but covers a broad range of high frequencies. The same also holds for the localization of $Lx(t, f)$ around (t, f). Also see Figure 2.3

Furthermore, the wavelet transform does not use a general function $\phi(\,\cdot\,; f)$ to analyze the signal, but instead uses a so called *wavelet*. A wavelet is a function ψ with finite energy that fulfills the *admissability condition* (Louis et al., 1998)

$$0 < c_\psi := \int \frac{\big(F\psi(\omega)\big)^2}{|\omega|}\,\mathrm{d}\omega < \infty. \tag{2.7}$$

It is common to set $\psi_a := S_a\psi$. Using this notation, equation (2.1) becomes for the wavelet transform

$$L_\psi x(t, a) = \int x(\tau)\overline{\psi_a(t-\tau)}\,\mathrm{d}\tau. \tag{2.8}$$

There is an infinite number of wavelets fulfilling the equation (2.7)[5]. In EEG analysis a common choice is the morlet wavelet, which is usually denoted as a

[5]Indeed, wavelets form a dense subset of $L^2(\mathbb{R})$ (Louis et al., 1998)

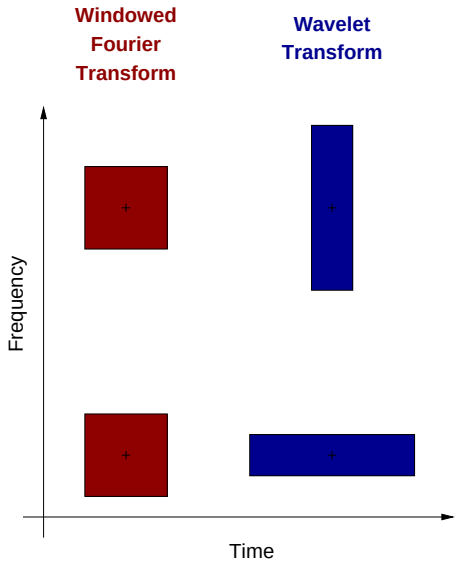

Figure 2.3.:
Localization properties of windowed fourier transform and wavelet transform. In the left part, the time-frequency localization properties of the windowed fourier transform are shown. In the right part, the time-frequency localization properties of the wavelet transform are shown. While the windowed fourier transform has the same localization properties for all frequencies, the wavelet transform adapts the window size to the analyzed frequency.

modulated Gaussian (Herrmann et al., 2005)

$$\psi(t) = A \exp\big(-\frac{t^2}{2}\big) \exp(2\pi\imath f_0 t), \tag{2.9}$$

with the real parameter A usually set such that ψ has unit energy. Careful evaluation of equation (2.7) shows that this is actually not a wavelet, because the integral does not converge. However, a slight modification of the modulation term from $\exp(2\pi\imath f_0 t)$ to $\exp(2\pi\imath f_0 t) - \kappa$, with $\kappa := \exp(-(2\pi f_0)^2/2)$ solves the problem analytically. The computations in this report are performed on the basis of equation (2.9), because κ will usually be very small ($< 10^{-8}$ for $f_0 = 1$).

The choice of a complex wavelet in equation (2.9) also results in a complex wavelet transform $L_\psi x$. This makes plotting $L_\psi x$ particularly difficult. In the next section we will derive three simple measures from the wavelet transform, that describe those characteristics of the event related EEG, that we will consider in the current report.

2.2.4. Statistical quantities to describe EEG signals in time and frequency

We will now consider a set of N EEG trials $X = \{x_n(t)\}_{n=1}^N$, that were recorded in a fixed relation to some stimulus of interest (suppose that $t \in [t_0, t_1]$, where $0 \in [t_0, t_1]$ is the time of the stimulus)[6]. For convenience, we will further denote the averaged ERP as

$$\bar{x}(t) = \frac{1}{N} \sum_{n=1}^{N} x_n(t).$$

[6]In practice the $x_n(t)$ will only be known at discrete sample time points t_k, $k = 0, \ldots, K$. The effects of such a sampling are described in detail in the book by Oppenheim et al. (2004).

A straight forward measure of event related oscillatory activity is[7]

$$\operatorname{evo} X(t,f) := |L_\psi \bar{x}(t,f)| = \big|\frac{1}{N}\sum_{n=1}^{N} L_\psi x(t,f)\big| \tag{2.10}$$

called *evoked activity* (Herrmann et al., 2005). Evoked activity represents the part of the event related activity, that is phase-locked to the stimulus. The evoked response defined in section 1.3 on page 5 is best detected using the measure of evoked activity.

In section 1.3, we also observed that not all event related activity needs to be phase-locked to the stimulus. A stimulus can also induce changes of the envelope activity without significantly altering the distribution of phases. To track this kind of changes a simple modification of equation (2.10) yields the *total activity* (Herrmann et al., 2005)

$$\operatorname{tot} X(t,f) := \frac{1}{N}\sum_{n=1}^{N} |L_\psi x_n(t,f)|. \tag{2.11}$$

Note that some authors also analyze evoked and total *power* (e.g. Tallon-Baudry et al., 1996b). These measures are in virtually all cases equivalent. Total activity contains contributions from both, phase-locked as well as non phase-locked components of the event related activity. Both evoked, as well as induced oscillatory responses can be observed as changes of total activity. However, the induced response will not be visible in evoked activity.

Due to the triangle inequality, the general relation $\operatorname{evo} X(t,f) \leq \operatorname{tot} X(t,f)$ holds. Here equality implies that the signals are perfectly phase-locked. To quantify the amount of phase-locking to the stimulus, an obvious measure would thus be:

$$P := \frac{\operatorname{evo} X(t,f)}{\operatorname{tot} X(t,f)}$$

For perfect phase-locking across trials, one would obtain $P = 1$ and otherwise a value between 0 and 1. Unfortunately the phase of high amplitude signal components will contribute more to this value, than the phase of low amplitude signals, because the phase of the single trials x_n is weighted by the amplitude in each single trial. If phase and amplitude are independent, this does not make a difference. Otherwise, however, the amount of phase-locking might be underestimated and amplitude outliers might obscure the pattern of phase-locking (e.g. Nolte et al., 2004). A measure, that is less prone to amplitude outliers has successfully been applied by Tallon-Baudry et al. (1996b). For a sample of phases, it is known in

[7] In this section we use the notation $L_\psi x(t,f)$ to denote the wavelet transform as in (2.8) with the wavelet scaled to be most concentrated around the frequency f. For the morlet wavelet (2.9) with $f_0 = 1$ this means $a = f^{-1}$.

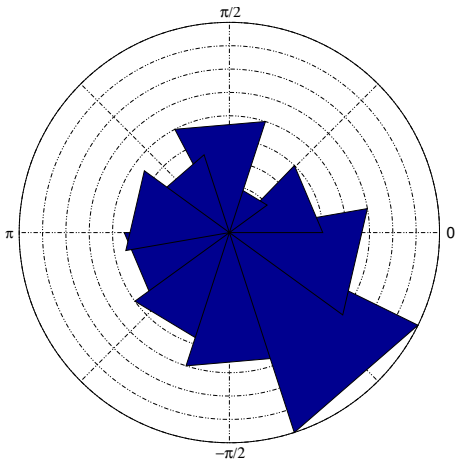

Figure 2.4.:
Distribution of phase angles for the evoked γ band response. Phases have been computed using the wavelet transform at the frequency of the evoked response. The histogram has been computed from 100 trials after stimulation with a grating pattern with a spatial frequency of 1 cycle per degree visual arc. (Data were taken from Fründ et al. (2007))

circular statistics as mean resultant length (Fisher, 1993). In our time-frequency notation it is defined by

$$\text{plf}\, X(t,f) = \Big|\frac{1}{N}\sum_{n=1}^{N}\frac{L_\psi x_n(t,f)}{|L_\psi x_n(t,f)|}\Big|. \tag{2.12}$$

To distinguish the measure (2.12) that varies in time and frequency from mean resultant length derived from a fixed sample of phases, and to relate our results to data from other groups, we will here use the term *phase-locking factor*. A value $\text{plf}\, X(t,f) = 1$ implies perfect phase-locking with all trials having the same phase. Unfortunately a value $\text{plf}\, X(t,f) = 0$ does not necessarily imply a uniform distribution of phases. This further requires the distribution of phases to be unimodal (Fisher, 1993). Surprisingly there seem to be no studies that systematically investigate the phase distribution of stimulus related EEG γ oscillations. Nunez & Srinivasan (2006, p. 459) present histograms of phases in the θ range (5-7 Hz) that are clearly unimodal. Unsystematic inspection of γ band phase histograms suggests, that unimodality is at least approximately fulfilled for γ band responses too (also see Figure 2.4).

2.2.5. Definitions of evoked and induced GBR

Based on the statistical quantities introduced in section 2.2.4 on page 20, more quantitative definitions of the concepts of evoked and induced GBR can be formulated. A significant deflection of γ activity from a prestimulus baseline will be termed a γ *band response* (GBR). We will differentiate two types of GBRs

1. An *evoked GBR* (eGBR) is characterized by an increase of evoked γ band activity and the phase-locking factor.

2. An *induced GBR* (iGBR) is characterized by an increase of total γ band activity without an accompanying increase of the phase-locking factor.

We will usually further constrain our definitions of eGBR and iGBR by accepting only responses from a certain time and/or frequency range.

The frequencies of GBR show considerable inter individual variability (Busch et al., 2004). Therefore, averaging the time frequency representations of evoked activity, total activity and phase-locking factor will generally smear the responses in frequency. To avoid such smearing effects, we determined the responses individually from every participant and display the time courses of the respective measure at the frequency of the GBR (i.e. at the peak in the time frequency plane).

2.3. Outline for the following experiments

In the following three chapters (3 on page 25, 4 on page 37, and 5 on page 51), we will present empirical results from three different experiments.

In the first of these experiments (Chapter 3), we test the stability of large scale γ band oscillations over time. Only oscillatory responses with temporally stable properties can form a reliable control signal for timing based neural codes. Thus, establishing the temporal stability of evoked γ band responses constitutes a necessary condition for the following experiments.

As mentioned in Chapter 1, such temporal codes seem to be particularly important to achieve the speed of visual processing. If evoked γ band responses help to quickly establish a framework for reliable processing on the basis of such temporal codes, one should expect faster processing to be accompanied by elevated evoked γ band responses. This hypothesis is tested in the second experiment which is presented in Chapter 4.

In Chapter 4, we demonstrate that spontaneous fluctuations of reaction time can be associated with different levels of stimulus evoked γ band responses. However, can these responses be adapted to different situations? In the third experiment (Chapter 5), we go further into this question by contrasting situation in which participants have to either respond as quickly as possible to a visual stimulus or have to wait for a certain amount of time until they may respond to the stimulus. If evoked γ band responses form a basis for rapid, timing based processing, they should be facilitated in the former case of speeded processing. If processing is adapted to the demands of the current task, evoked γ band responses should additionally be diminished in the case of a delayed response.

3. Experiment I: evoked γ band responses are test retest reliable

The experiment described in this chapter has been published as in the Journal "Clinical Neurophysiology" (Fründ et al., 2007).

3.1. Introduction

In section 1.2 on page 4, large scale brain oscillations have been introduced as a possible control signal for fast temporal coding schemes based on spiking neurons. In particular, such a control signal should reliably be reset following suffciently large changes of the input (Kupper et al., 2005).

γ oscillations have recently been related to pathological brain function (see Herrmann & Demiralp, 2005, for a review). γ oscillations seem to be related to a variety of neuropsychiatric disorders such as schizophrenia (Lee et al., 2003, 2001; Basar-Eroglu et al., 2006), attention-deficit hyperactivity disorder (ADHD; Yordanova et al., 2001), or autism (Grice et al., 2001; Brown et al., 2005). It seems reasonable to also use oscillatory brain responses in the γ range as a diagnostic tool for neuropsychiatric disorders (Spencer et al., 2003; Ribary et al., 1991). A prerequisite for such clinical application as well as for our following experiments would be that γ band responses (GBRs) can reliably be detected such that variations in the GBR could be related to specific longer lasting aspects of brain function rather than random or transient variations. Along these lines Debener & Engel (2005) have recently commented a review on γ activity in neuropsychiatric disorders (Herrmann & Demiralp, 2005) that the reliability of γ responses needs to be demonstrated before they can be used for clinical diagnosis.

GBRs can be measured from a wide variety of brain structures (Basar et al., 2001). As mentioned in section 1.3 on page 5, two types of GBRs are usually distinguished: Evoked GBRs (eGBRs) are phase-locked to the onset of a stimulus and do not necessarily correspond to amplitude modulations in the single trials, whereas induced GBRs (iGBRs) usually occur in a later time window and are not time locked to the onset of a stimulus (Basar-Eroglu et al., 1996). Induced GBRs are usually detected as amplitude modulations in single trials, and are now commonly related to a wide variety of cognitive processes (Engel et al., 2001; Tallon-Baudry & Bertrand, 1999; Keil et al., 2001) as well as certain types of learning and memory (Gruber & Müller, 2005, 2006). Most researchers agree

in that the earlier eGBRs depend on stimulus factors such as size, eccentricity (Busch et al., 2004), or spatial frequency (Fründ et al., 2007). However, they also seem to be modulated by basic cognitive processes such as memory matching (Herrmann et al., 2004) or attention (Busch et al., 2006; Tiitinen et al., 1993; Debener et al., 2003; Fell et al., 2003). Whereas the reliability of iGBRs has been shown before (Keil et al., 2003; Hoogenboom et al., 2006), such demonstrations lack for the eGBR.

In the current study we investigated the test-retest reliability of eGBRs in response to sinusoidal gratings. Since a recent study revealed that size matters for evoking γ activity (Busch et al., 2004), we used stimuli of different size for our test.

3.2. Methods

3.2.1. Participants

Twelve healthy volunteers aged between 20 and 44 years (mean age 27 ± 6.721, 5 m, 7 f) participated in the current study. We decided that 12 participants would be enough to get an idea of the reliability of eGBRs. However, due to the small sample size, the results remain preliminary. All participants had normal or corrected to normal vision and were free of current or past neurological or psychiatric disorders. Before the first recording session started, participants gave their informed consent. The experimental procedure was in accordance with the guidelines of the local ethics commitee of the university of Magdeburg and the declaration of Helsinki.

3.2.2. Stimuli and experimental procedure

All participants took part in two recording sessions, temporally separated by two weeks. During both recording sessions the participants had to perform the same task.

The task of the participants was to detect the orientation of monochromatic gratings with a spatial frequency of 2 cycles per degree visual arc (cpd) and a Michelson contrast of 50%. These gratings were either rotated 45 degree clockwise from a vertical orientation or counterclockwise. Examples of the stimuli can be found in Figure 3.1 on the facing page. Participants indicated the detected orientation by pressing a button with one hand or another button with the other hand. The gratings subtended either 10 degree visual arc (big stimuli) or 1.3 degree (small stimuli). This results in 4 different stimuli, each of which was presented 100 times. Thus, in total the participants perceived 400 grating patterns during the experiment.

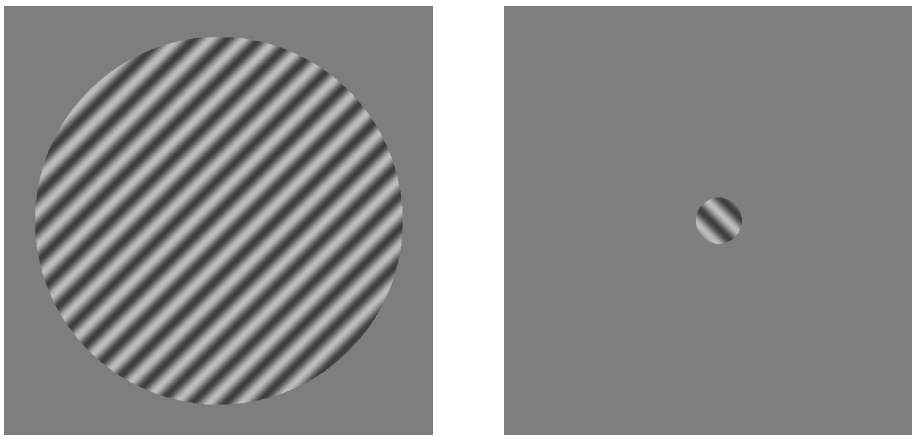

Figure 3.1.:
Examples of the stimuli used in the experiment. Left: big stimulus, right: small stimulus

Response hands were counterbalanced across participants but remained constant during the two sessions. The stimuli were presented on a TFT monitor (width = 34.5 cm, height = 25.9 cm) placed at a distance of 110 cm in front of the participants. Monitor refresh rate was 75 Hz. Participants were instructed to fixate a small white cross in the center of the screen during the whole experiment. Furthermore, electrooculographic (EOG) activity (see Section 3.2.3) was recorded in order to discard trials that were contaminated with eye movements. Stimuli were presented for 1000 ms with inter stimulus intervals varying randomly between 1000 ms and 2000 ms.

3.2.3. Data acquisition

During data recording, participants sat in an electrically shielded and sound attenuated room (IAC, Niederkrüchten, Germany). The stimulation monitor was placed outside the recording cabin behind an electrically shielded window. All devices inside the cabin were battery operated to avoid line frequency interference (50 Hz). EEG activity was measured from 31 scalp locations according to an extended 10-20 system. The nose served as reference. Electrooculographic activity was measured from an electrode placed below the orbital rim in order to detect artifacts due to eye movements. Activity was recorded using sintered Ag/AgCl electrodes mounted in an elastic cap (Easycap, Falk Minow Services, Munich, Germany) and amplified by means of a BrainAmp amplifier (Brain Products, Munich, Germany). Electrode impedances were kept below 5 kΩ. The EEG signals were filtered between 0.02 and 250 Hz, digitized at a rate of 500 Hz and stored on a computer hard disc for offline analysis. Digitized EEG data were transferred to a computer outside the recording cabin with a fiber optic cable. The data were dig-

itally high-pass filtered offline with a cutoff frequency of 0.5 Hz in order to avoid slow shifts in the baseline. An automatic artifact rejection was computed which excluded trials from further analysis if the standard deviation within a moving 200 ms time window exceeded 40 µV in one channel. The automatic artifact rejection was supplemented by visual inspection to ensure that only trials without artifacts were included in the subsequent analysis. After artifact rejection on average 165 trials per session per subject went into the analysis.

3.2.4. Data analysis

In order to obtain a time frequency representation of the EEG signals, a wavelet transform was performed as described in Section 2.2 on page 17. At 40 Hz the wavelet had a time resolution of $2\sigma_t = 50$ ms and a frequency resolution of $2\sigma_f = 13$ Hz. The exact time frequency resolution of the wavelet depended on the analyzed frequency. The wavelets were normalized to have unit energy. From the wavelet transformed data the three measures described in Section 2.2.4 on page 20 were derived: (i) the amount of evoked activity, (ii) the total γ activity and (iii) the phase-locking factor. This resulted in a representation of the responses of every participant in the plane spanned by time and frequency, where the frequency of the participant's response could be analyzed as well as the magnitude of the response at that frequency. From the time frequency planes for evoked and total activity, the average from a baseline 200 to 100 ms before stimulus onset was subtracted.

In a previous study we reported strong eGBRs over posterior electrodes O1, O2, P3, Pz and P4 (Busch et al., 2006). This was confirmed by the current results. We therefore decided to average the time frequency planes from these electrodes to quantify eGBRs. Response frequencies were defined for each condition in the time frequency plane averaged accross electrodes O1, O2, P3, Pz, and P4[1] as those frequencies between 28 and 90 Hz that showed the strongest increase in the time range between 50 and 130 ms after stimulation onset with respect to a baseline level (100 to 200 ms before stimulus onset). The time course of the γ band response was computed as the average of the time courses at these individually defined response frequencies. Thus, we acquired one time course for evoked, one for total activity and one for phase-locking. If a participant did not show a dominant response peak but rather multiple small peaks that could not be distinguished from noise, this response was excluded from the reliability analysis of response frequencies. Examples for this procedure are illustrated in Figure 3.2.

From the time courses we obtained the peak magnitude in the time window between 50 and 130 ms after stimulation onset. If for a particular condition no response frequency could be ascertained, the peak magnitude was extracted

[1] Reliabilities of eGBR derived from single channels were generally smaller (by a value of approximately 0.2 for big stimuli) and less significant ($0.05 > p > 0.03$)

at the response frequency of the other condition (big or small respectively). If a response frequency could not be ascertained for the other condition either, peak magnitude was extracted at 40 Hz. This procedure yields different analysis frequencies for eGBR, phase-locking and total GBR. However, the differences in analysis frequencies were well below the bandwidth of the employed wavelets.

Thus, for every session we analyzed 6 response frequencies and response magnitudes (two conditions: small, big stimulus; three characteristic values: evoked activity, total activity, phase-locking). In order to obtain a measure for test-retest reliability, the correlation for all these values was derived separately between the first and the second session (Keil et al., 2003). The correlations were tested by means of a t-test with $n - 2$ degrees of freedom, where n denotes the number of participants that were included in the analysis. The statistics were performed using the function `cor.test()` from the statistical analysis software "R" (R Development Core Team, 2004).

To get an estimate of the reliability within a single session, we randomly split the trials from the first session into two subsets. These two subsets were compared in the same way as the data from the two sessions.

3.3. Results

For big stimuli a marked eGBR could be observed at posterior electrodes. This was not the case for small stimuli. Figure 3.2 shows time-frequency representations of the evoked γ response from two participants. Figure 3.3 displays topographies of the responses to big and small stimuli.

3.3.1. Behavioral data

Mean reaction times were 477 ± 65 ms. For both stimuli the mean reaction times were highly correlated between sessions (big stimuli: $r = .91$, $t_{10} = 6.95$, $p < 0.0001$, small stimuli: $r = .89$, $t_{10} = 6.02$, $p < 0.001$).

3.3.2. Evoked GBR

Response frequencies of evoked activity significantly correlated for the big stimulus ($r = .85$, $t_{10} = 5.1$, $p < 0.001$). For the small stimulus, the number of responses for that a response frequency could be distinguished (5) was too small to calculate a meaningful correlation. Response magnitudes of evoked activity were significantly correlated only for the large stimulus ($r = .82$, $t_{10} = 4.55$, $p < 0.01$), but not for the small stimulus ($r = .30$, $t_{10} = 1.1$). Scatter plots of the response frequencies and magnitudes of the eGBR can be found in Figure 3.4. A comparison between first and second session for big and small stimuli from two representative subjects is presented at the top of Figure 3.2.

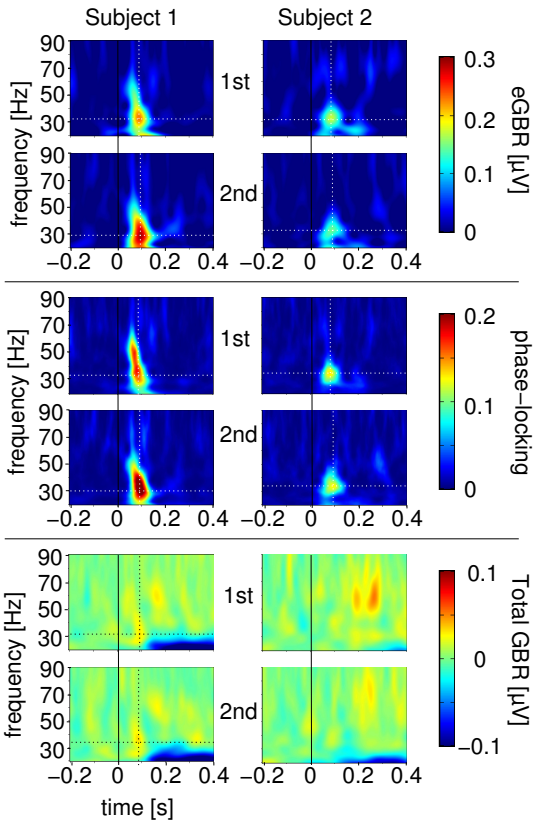

Figure 3.2.:

Time-frequency representations of evoked activity (top), phase-locking (middle) and total activity (bottom) in response to the big grating stimulus from two single representative participants. In every display two time-frequency plots are shown. The first corresponds to the first session, the second to the second session. To obtain these time-frequency representations, the time-frequency representations from electrodes O1, O2, P3, Pz, P4 have been averaged. Dotted lines indicate the time-frequency position at which the values were extracted for further computation. Plots of evoked activity and phase-locking show a high reliablity across sessions, while this was less clear for total activity. Note that for subject 2 no response frequency for total activtiy was ascertained in the early time window. Subject 2 was the only subject that displayed a late total GBR. This was, however, not test-retest reliable.

Figure 3.3.:
Evoked GBR in response to big stimuli (left column) and small stimuli (right column). Top: Time courses at electrode O2, solid lines represent responses from the first session, dotted lines represent responses from the second session, middle: topographies from first session, bottom: topographies from second session. Data were averaged accross all participants. Topographies correspond to the time window 60 to 115 ms after stimulus onset. Both time courses and topographies in response to big stimuli were highly reliable across sessions.

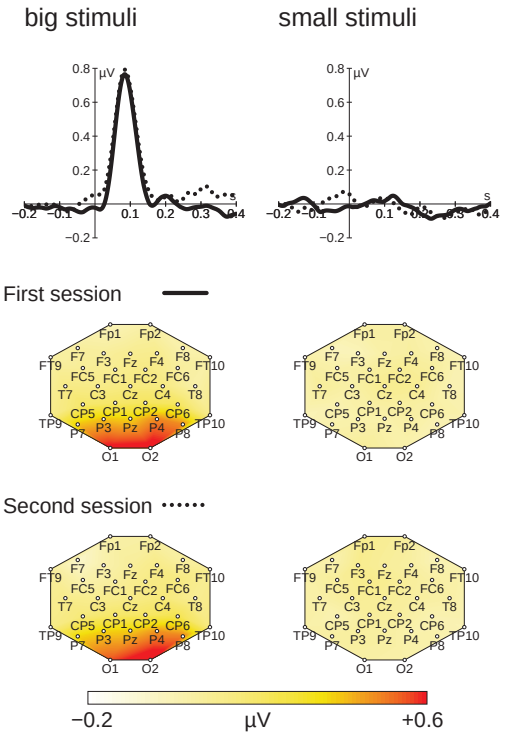

Table 3.1.:
Correlations between first and second session, evo X indicates evoked activity, plf X indicates phase-locking and tot X indicates total activity. Note that frequency was assumed to be 40 Hz for the magnitude analysis if no clear peak was visible. However, frequency could not be analyzed in these cases.

	big stimuli			small stimuli		
	Correlation r	t value	p value	Correlation r	t value	p value
Response frequencies						
evo X	0.85	5.1	0.001	not enough observations		
plf X	0.95	8.95	0.0001	not enough observations		
tot X	not enough observations			not enough observations		
Response magnitudes						
evo X	0.82	4.55	0.01	0.30	1.1	n.s.
plf X	0.88	5.98	0.001	0.21	0.64	n.s.
tot X	0.31	0.99	n.s.	0.49	1.67	n.s.

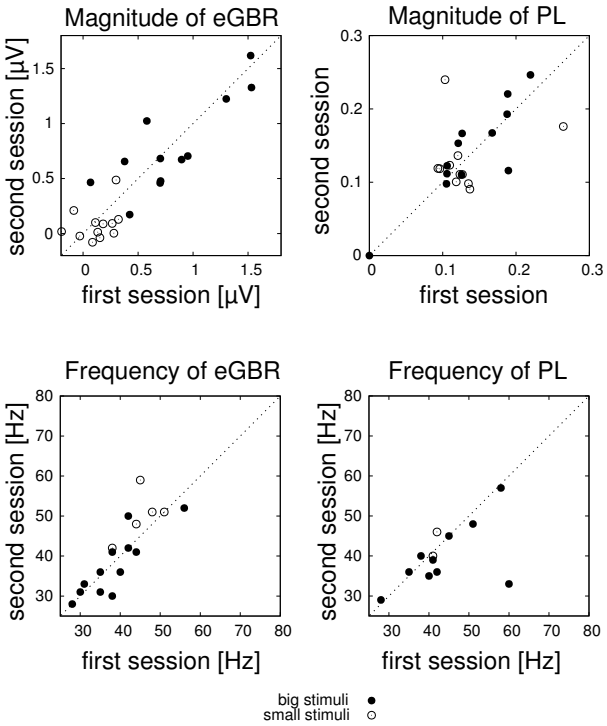

Figure 3.4.:
Scatter plots of evoked responses. Top: response magnitudes, Bottom: response frequencies. Left: Magnitude and frequency of evoked γ band response, right: magnitude and frequency of phase-locking. Filled circles represent responses to big stimuli, open circles represent responses to small stimuli. In all plots high reliablity across sessions can be observed for big but not for small stimuli.

3.3.3. Phase-locking

Phase-locking revealed an even larger correlation across sessions, than did the evoked activity. Response frequencies as well as magnitudes for the big stimuli were highly correlated (response frequencies: $r = .95$, $t_8 = 8.95$, $p < 0.0001$, response magnitudes: $r = .88$, $t_{10} = 5.98$, $p < 0.001$). For small stimuli response frequencies could only be distinguished in five participants which precluded the calculation of a meaningful correlation. Magnitudes of phase-locking in response to small stimuli were not significantly correlated ($r = .21$, $t_9 = 0.64$). Scatter plots of frequencies and magnitudes of phase-locking are presented in the right column of Figure 3.4. Time frequency representations of the responses from two representative subjects are compiled in the middle panel of Figure 3.2.

3.3.4. Total γ activity

Response frequencies of total γ activity could only be ascertained for three participants. Time frequency planes from other participants did not show a clear peak at any frequency. This precluded the calculation of a meaningful correlation of response frequencies. The magnitudes of total γ activity were not significantly correlated ($r < .5$, $t_9 < 1.7$). Total γ activity was not significantly correlated in later time windows either. Time frequency representations of the responses from two representative subjects are displayed at the bottom of Figure 3.2.

3.3.5. Event-related potentials

Event-related potentials (ERPs) are plotted in Figure 3.5. Although we did not analyze ERP components statistically, two aspects can be noted about the ERP. First, the early responses to big as well as small stimuli are very similar across sessions. Second, in line with previous findings (Debener et al., 2002) the later responses to big stimuli are slightly more similar between sessions, than are those to small stimuli.

3.3.6. Split-half reliabilities

The results of the split-half analysis were comparable to those from the test-retest analysis. For big stimuli both, frequency as well as magnitude of the eGBR were significantly correlated (big stimuli: frequency: $r = .89$, $t_8 = 5.54$, $p < 0.001$, magnitude: $r = .80$, $t_{10} = 4.29$, $p < 0.01$), whereas this was not the case for small stimuli (frequency could only be ascertained in five participants, magnitude: $r = -.51$, $t_{10} = -1.87$). High correlations were obtained also for phase-locking (big stimuli: frequency: $r = .78$, $t_6 = 3.07$, $p < 0.05$, magnitude: $r = .80$, $t_{10} = 4.18$, $p < 0.01$, small stimuli: frequency could only be ascertained in four participants, magnitude: $r = -.04$, $t_{10} = 0.12$), but not total γ activity

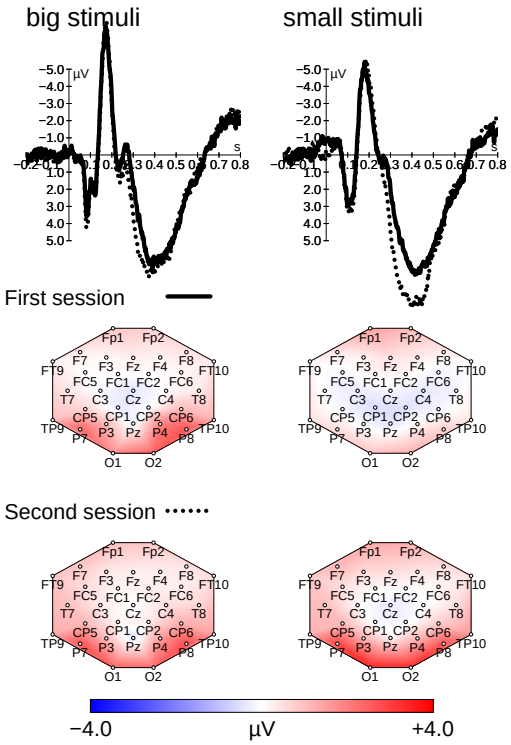

Figure 3.5.:
Event-related potentials after stimulation with big stimuli (left column) and after stimulation with small stimuli (right column). The top row shows time courses of the event-related potential, the second row shows topographic maps of activity between 80 and 120 ms in the first session and the third row shows topographic maps of the same time window in the second session. ERPs were lowpass filtered at 20 Hz for display.

(big stimuli: frequency could only be ascertained in five participants, magnitude: $r = .45$, $t_{10} = 1.59$, small stimuli: frequency could only be ascertained in five participants, magnitude: $r = -.73$, $t_{10} = -3.43$)

3.3.7. Reliabilities of broad band γ activity

We performed the same analysis as above with the amplitudes averaged across the whole time-frequency range of interest (50-130 ms, 28-90 Hz). Correlations were significant under the same conditions as with peak frequency analysis. However, these correlations were much lower (on average .17 less than for peak frequencies).

3.4. Discussion

In the current study we investigated the reliability of early, phase-locked γ activity in response to different stimulus sizes. We observed that for large stimuli a reliable measurement of longer lasting properties of evoked, phase-locked γ activity is possible. Total γ activity was not significantly correlated between the two sessions.

It has been demonstrated previously, that evoked γ oscillations are highly dependent upon parameters of the stimulation procedure like spatial frequency (Fründ et al., 2007), size or eccentricity (Busch et al., 2004). For small stimuli subtending only one degree visual arc, the eGBR hardly exceeds the noise level. We found the same in our current data and could even extend these findings by showing that for small stimuli stable detection of γ responses across two recording sessions is not possible either.

From the fact that phase-locking in our data was generally more reliable than total γ activity, we infer that the reliable part of the eGBR was due to phase-locking rather than modulation of amplitudes in single trials. This is in line with findings indicating that phase-locking and power modulations of early γ responses are independent parameters of cortical information processing (Yordanova et al., 1997; Fell et al., 2005). Total γ activity, was not significantly correlated between sessions. This might explain, why Keil et al. (2003) found only weak reliabilities for power increases of early γ band responses.

Phase-locked γ activity has been regarded as being mainly related to sensory processing (Karakaş & Başar, 1998), which is modulated by top-down processes like memory (Herrmann et al., 2004) or attention (Busch et al., 2006; Tiitinen et al., 1993; Debener et al., 2003; Fell et al., 2003). Phase dynamics of high frequency brain oscillations have gained interest in recent years (Makarenko & Llinás, 1998; Kazantsev et al., 2004; Freeman & Rogers, 2002). The phase of ongoing oscillations in the γ-β range is spontaneously reset at a frequency of approximately 5 Hz (Freeman & Rogers, 2002). These authors observed that phase-resets occur simultaneously at different spatial scales of cortical processing

and can be very rapid. Such phase-resets have been studied in much detail in the inferior olive. The subthreshold oscillations of neurons in the inferior olive can be reset rapidly to a value that is determined by properties of the stimulus (Kazantsev et al., 2004). Makarenko & Llinás (1998) suggested that such mechanisms might be found in different brain structures in which subthreshold oscillations can be detected. Thus, it might be possible, that resetting the phase of ongoing high frequency oscillations provides a mechanism for rapid classification of visual stimuli, (Körner et al., 1999). These authors further argue, that for the very same oscillation phase-locking to the stimulus might become weaker with time, while the cells are synchronized to each other by a common subthreshold oscillation. From this point of view it seems reasonable to expect phase-locking to be reliable in an early time window, whereas amplitudes (i.e. local synchronization between many neurons) become more reliable in later time windows as has been shown before (Hoogenboom et al., 2006; Keil et al., 2003).

In a line of experiments, we studied the conditions for the detection of eGBRs. We especially reported that measurement of eGBRs is only possible, if the stimulation is appropriate (Busch et al., 2004, 2006; Fründ et al., 2007). The current results extend these findings by demonstrating that γ oscillations can also be reliably detected if the stimulation is appropriate. Thus, a clinical application of eGBRs as a diagnostic tool seems realistic. Especially schizophrenia has been associated with abnormalities of γ oscillations (Lee et al., 2003). For schizophrenic patients deficits in early visual processing have been demonstrated (Brand et al., 2005), that could also account for cognitive impairments in higher order processes like social cognition (Sergi & Green, 2002). It has been argued that these deficits in early visual processing could be explained by dysfunction of the magnocellular pathway in schizophrenic patients (Schechter et al., 2005). It has been suggested that GBRs can be associated with activity in the magnocellular pathway (Sewards & Sewards, 1999). Indeed it was reported that phase-locking of oscillatory γ activity is abnormal in schizophrenic patients and that these abnormalities are correlated with symptoms of schizophrenia (Spencer et al., 2003, 2004). The current findings might thus be speculated to open new paths for a diagnosis of magnocellular dysfunction in schizophrenia. However, to date no specific links between eGBRs and magnocellular function have been established.

We conclude that using appropriate stimulation it is possible to obtain reliable measurements of evoked, phase-locked γ oscillations in EEG measurements.

4. Experiment II: γ band responses vary with reaction time

The results of this experiment have been published in the Journal "BMC Neuroscience" (Fründ et al., 2007).

4.1. Introduction

As noted in chapter 1 on page 1, response times to visual stimuli can be extremely fast in some cases. However, there is also considerable intra-individual variability in response times across trials, even under identical experimental conditions. Which neural processes can account for these behavioral differences? Why do we manage to be fast on some trials but not on others?

Experimental findings suggest that processing of visual information may be extremly rapid, leaving an upper limit of 10-20 ms for information transfer between two neurons at successive levels of the visual processing hierarchy (Thorpe et al., 1996). This implies that processing must be achieved using the very first spikes of a neuronal stimulus response based on an ensemble code rather than a rate code (Thorpe et al., 2001, also see section 1.1 on page 1). Such effective and fast transfer demands synchronous arrival of several spikes at the same target neuron, propagated from different source neurons that were activated by the respective stimulus. However, the membrane potential of neurons is randomly fluctuating around its resting potential. Therefore, without a synchronization of those fluctuations even a coherent wave of input spikes to a certain processing stage will result in an increasingly scattered spike distribution at the input to the next processing stage. In this case reliable processing of a stimulus can only be achieved based on a time consuming rate code. Rodemann & Körner (2003) demonstrated in a neural network simulation that stimulus-locked, evoked γ band responses (eGBRs) can be the expression of a phase reset of ongoing neuronal activity after a visual stimulus, which results in strong synchronization of spiking activity in the stimulated neuronal population. In this case processing of the stimulus can be based on instantaneous evaluation of an ensemble code, which results in much faster responses.

As outlined in section 1.4 on page 9, eGBRs have so far mainly been studied in perceptual tasks in both auditory (Yordanova et al., 1997; Tiitinen et al., 1993) and visual modalities (Busch et al., 2004; Spencer et al., 2004). In these experi-

ments it could be shown that although eGBRs are highly dependent on physical parameters of the stimulation (Busch et al., 2004; Karakaş & Başar, 1998), they are significantly modulated by top down factors like attention (Busch et al., 2006; Tiitinen et al., 1993) or memory (Herrmann et al., 2004). Although the early time window in which they occur and the simulation performed by Rodemann & Körner (2003) render eGBRs a possible mechanism for fast response initiation, studies that link eGBRs and response times are rare. There is only indirect evidence regarding this topic. In studies investigating eGBRs in schizophrenic patients, decreased phase-locking is accompanied by prolongated reaction times in patients compared to healthy controls (Spencer et al., 2003). Furthermore, studies that investigated stimulus induced amplitude modulations in the γ range found relations between such amplitude modulations and reaction time (Haig et al., 1999; Jokeit & Makeig, 1994). Such later amplitude modulations of oscillations in the γ range, so called induced γ oscillations (Basar-Eroglu et al., 1996) have been associated with a wide range of cognitive processes (Tallon-Baudry et al., 1998; Engel et al., 2001) and learning (Gruber & Müller, 2005, 2006).

In the current study, we directly investigated the idea that phase-locked, evoked GBRs are relevant for speeded responses. Participants were asked to respond as fast as possible to large black squares presented on a white screen, while their electroencephalogram (EEG) was recorded. Trials in which the participants were able to respond fast were analyzed separately from trials with slower reactions. We hypothesized that eGBRs would be enhanced in those trials, in which the participants were able to respond fast, compared to trials, in which participants responded slower. We further explored whether these effects could be explained by amplitude modulations in the single trials or whether they were due to an increase in phase-locking to the onset of the stimulus.

4.2. Methods

4.2.1. Participants

Thirteen healthy volunteers aged between 22 and 44 years (mean age 27±6.7, 6m, 7f) participated in the current study. All participants had normal or corrected to normal vision and were free of current or past neurological or psychiatric disorders. Before the recording session started, participants gave their informed consent to participate. The experimental procedure was in accordance with the guidelines of the local ethics commitee of the university of Magdeburg and the declaration of Helsinki.

4.2.2. Stimuli and experimental procedure

The participants viewed large black squares (16×16 cm at a distance of 120 cm, subtending 8 degree visual arc) that were presented in front of a white background on a TFT monitor (width= 34.5 cm, height= 25.9 cm). Stimuli were presented for 1000 ms. The participants were instructed to press a button as fast as possible, as soon as a square appeared on the screen. After every button press, the participants received feedback about their reaction time. Stimuli were presented in three blocks of 200 trials each. Inter stimulus intervals (ISIs, time interval between offset of one stimulus and onset of the next stimulus) were taken from a uniform random distribution in one block, from a normal distribution in another block and from a shifted exponential distribution in the third block, to control anticipatory effects due to the randomization of the ISI. It has been shown, that stimulus preceding negative potentials are weakest for a uniform distribution of ISIs (Trillenberg et al., 2000). In all blocks mean ISI was 1200 ms and standard deviation was 300 ms. Block sequence and response hands were counterbalanced across participants. Participants were instructed to fixate a small black cross in the center of the screen during the whole experiment.

4.2.3. Data acquisition

During data recording, participants sat in an electrically shielded and sound attenuated room (IAC, Niederkrüchten, Germany). The stimulation monitor was placed outside the recording cabin behind an electrically shielded window. All devices inside the cabin were battery operated to avoid line frequency interference (50 Hz in Germany). EEG activity was measured form 31 scalp locations referenced to the nose. Electrode positions were selected according to an extended 10-20 system. Electrooculographic activity was recorded from an electrode placed below the orbital rim in order to detect eye movement artifacts. Activity was recorded using sintered Ag/AgCl electrodes mounted in an elastic cap (Easycap, Falk Minow Services, Munich) and amplified by means of a BrainAmp amplifier (Brain Products, Munich). Electrode impedances were kept below 5kΩ. The data was analog low pass filtered at 200 Hz, digitized at a rate of 500 Hz and stored on a computer hard disc for offline analysis. Digitized EEG data was transferred to a computer outside the recording cabin with a fiber optic cable. No analog or digital high pass filter was applied to preserve DC components of the signal. An automatic artifact rejection was performed which excluded trials from further analysis if the standard deviation within a moving 200 ms time window exceeded 40 μV in any channel (EEProbe, ANT, Enschede). The automatic artifact rejection was supplemented by visual inspection to ensure that only trials without artifacts due to eye movements, motor activity or amplifier noise were included in the subsequent analysis.

4.2.4. Data analysis

For each single trial the response time was recorded. Based on inspection of the response time histograms, only responses between 100 and 400 ms were considered for further analysis. See top of Figure 4.4 on page 45 for a histogram of response times accross all participants. To investigate the current hypotheses it might sound obvious to perform a correlational analysis. One would expect, that there is a high correlation between the reaction time and the eGBR (and probably the slow negative potential) across trials. The main problem with this approach lies in the definition of evoked activity. Evoked activity is defined as being phase-locked to the onset of the stimulus (Basar-Eroglu et al., 1996). Unfortunately phase-locking to the onset of a stimulus cannot be analyzed in single trials. Thus, a correlational analysis of the observed effects could only indirectly be performed on the basis of subaverages. To this end, responses of each participant were split into two groups according to whether the response was faster than the participant's median response time or slower.

As neither EEG nor response time data differed significantly between blocks, data from all three blocks were merged for the analysis of EEG. Event-related potentials (ERPs) were computed as averages across trials for fast response and slow response trials separately. To investigate the impact of slow ERP components preceding the stimulus on eGBRs, a straight line was fit to the last 500 ms before stimulus onset in single trials. Based on the slope of this line a median split was performed to obtain trials with strong stimulus preceding negativity and weak stimulus preceding negativity.

To analyze event-related γ oscillations, a wavelet transform was applied (see section 2.2 on page 17 for a detailed description). The wavelet transform was computed at linearly spaced time and frequency positions using a discrete version of the integral wavelet transform with the morlet wavelet (i.e. a modulated gaussian) as basis function. At 40 Hz this wavelet had a time frequency resolution of $2\sigma_t \approx 50$ ms and $2\sigma_f \approx 13$ Hz. The exact time frequency localization depends on the analyzed frequency. The wavelet transform represents a signal as a function of time and frequency. From these time-frequency representations the three characteristic values described in Section 2.2.4 were derived: (i) the strength of the evoked activity, (ii) total activity (iii) the phase-locking factor (PLF). On average 130 trials were included in the analysis of ERP and oscillatory activity for fast and slow response subaverages. For a uniform distribution of phases across trials the 95th percentile of the phase-locking value was numerically estimated to be ≈ 0.15.

From the time frequency representations of evoked activity and total activity, the average activity from the last 200 ms before stimulus onset was subtracted, to obtain a measure of the event related changes of these quantities.

One participant was excluded from the GBR analysis due to large muscular artifacts that could not be separated from the GBR.

Table 4.1.:
Response frequencies and latencies for different participants. If a participant did not show any peak at all, this value is marked as "no response" in the table and the value was excluded from the statistical analysis

participant	early (60-140 ms)		late (180-400 ms)	
	frequency [Hz]	latency [ms]	frequency [Hz]	latency [ms]
participant 1	33	140	53	336
participant 2	31	120	no response	
participant 3	33	99	45	328
participant 4	37	69	52	268
participant 5	35	137	42	331
participant 6	38	96	40	294
participant 7	39	90	48	311
participant 8	30	97	40	304
participant 9	33	113	49	279
participant 10	36	72	53	255
participant 11	42	130	44	218
participant 12	61	79	44	300
participant 13	excluded due to high frequency artifacts			

For every participant the eGBR was defined as the peak response in a frequency range between 30 and 90 Hz and a time range between 50 and 160 ms after stimulation onset. The frequency range for the eGBR was predefined to include the whole γ frequency range. The time range was adapted to include all initial phase-locked responses (see Table 4.1).

The analysis was focused on peak responses, because the response frequency in the γ range has been shown do vary considerably across participants (Busch et al., 2004). Furthermore, the data from Chapter 3 demonstrated that peak responses are more reliable than averages across multiple frequencies. Responses were pooled into two regions of interest (ROI) as summarized in Table 4.2 on the next page. The posterior ROI was chosen to include channels over visual areas, the central ROI was chosen to include channels from a broad area around the central sulcus. We decided to select electrodes from both hemispheres into the ROI, because we observed in a pre-analysis, that no significant laterality effects were present in the data (slow negative potential: $t_{12} = .29$, central eGBR: $t_9 = -0.84$, contra- vs. ipsilateral to responding hand). Response strengths and latencies were analyzed by means of ANOVA for repeated measurements with two factors (ROI $\times$ SPEED). If for a particular participant and condition no response peak could be extracted, this value was considered "missing" in the statistical analysis.

The statistical analysis was performed separately for evoked activity, total

Table 4.2.: Regions of interest

ROI	channels
central	TP9, TP10, T7, T8, CP5, CP6, C3, C4, Cz, FC1, FC2, FC5, FC6
posterior	CP1, CP2, P3, P4, Pz, P7, P8, O1, O2

activity and phase-locking factor.

4.3. Results

4.3.1. Response times

Median response times ranged between 170 and 236 ms (mean=204 ms, standard deviation=16 ms). Mean response times for fast trials (faster, than the median response time, red) and slow trials (slower, than the median response time, blue) are indicated in Figures 4.1 on the facing page and 4.2 on page 44 as vertical dotted lines. A histogram of all response times can be found at the top of Figure 4.4 on page 45.

4.3.2. Event related potentials

A slowly increasing negative potential was observed preceding the stimulus. In order to test whether this negativity was influenced by the degree of expectancy of the next stimulus, we used three different randomizations of the inter stimulus interval (ISI): a uniform distribution, for which all possible ISIs had the same probability, a gaussian distribution with a clear peak for medium latency ISIs, an exponential distribution, for which very long ISIs are possible, but most ISIs are relatively short. These three ISI distributions have been shown to influence the slow stimulus preceding potentials (Trillenberg et al., 2000). In the current data, however, the negative potential did not differ between different randomizations of the inter stimulus interval ($F_{2,12} = 0.51$) and was most pronounced over central electrodes. Separating the trials into fast and slow responses revealed that this slowly increasing negative potential was large for fast response trials, but nearly absent for slow response trials (Fig. 4.1). Comparing the mean amplitude in the last 500 ms preceding stimulus onset in a central region of interest (ROI) yielded a highly significant difference ($t(12) = -6.233, p < 10^{-4}$).

In addition also a difference in P1-N1 peak to peak amplitude is visible in Figure 4.1. However, this difference was only visible in a small subset of three participants. In some participants no P1-N1 complex could be found or the effect was even reversed. A statistical analysis of those participants for which a P1-N1 pattern could be observed did not yield a significant difference between fast and slow responses ($t_{10} = -1.71$).

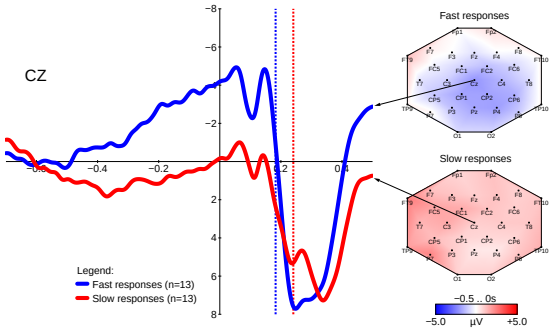

Figure 4.1.:
Averaged event related potentials for fast and slow responses (left) and topographic maps of the average activity in the time window -0.5 to 0 s. The stimulus was presented at 0 s. Dotted lines indicate mean response times of fast response trials (red) and slow response trials (blue). Note that the negative potential starting approximately 700 ms before stimulus onset for fast response trials is virtually absent for slow response trials.

4.3.3. γ band responses

A clear eGBR could be observed over posterior and central areas. This response peaked between 50 and 160 ms at frequencies between 30 and 50 Hz (see Table 4.1 on page 41). Evoked GBRs were generally more pronounced over the posterior ROI as compared to the central ROI ($F_{1,9} = 28.91, p < 0.001$). No significant differences for different ISI randomizations were found ($F_{2,9} = 0.29$). Separating the trials into fast and slow behavioral responses yielded a clear difference in the eGBR (see Fig. 4.2 on the following page): In trials with fast behavioral responses, eGBRs were larger in amplitude ($F_{1,9} = 12.36, p < 0.01$) and earlier in latency ($F_{1,9} = 5.54, p < 0.05$) than in trials with slow behavioral responses. No significant differences were observed in the baseline level of γ activity ($t_{11} = 0.36$).

We analyzed phase-locking factor and total activity patterns in the same time window to investigate whether the effects of evoked activity were due to an increased phase-locking to the stimulus or due to amplitude modulations in the single trials. Phase-locking was significantly enhanced for the fast response trials compared to the slow response trials ($F_{1,10} = 9.30, p < 0.05$, Fig. 4.3 on the next page). Phase-locking was also more pronounced over the posterior ROI as compared to the central ROI ($F_{1,10} = 11.63, p < 0.01$). Total activity was more pronounced over the posterior ROI ($F_{1,9} = 30.77, p < 0.001$), too. However, total activity between 50 and 160 ms did not depend on the response speed

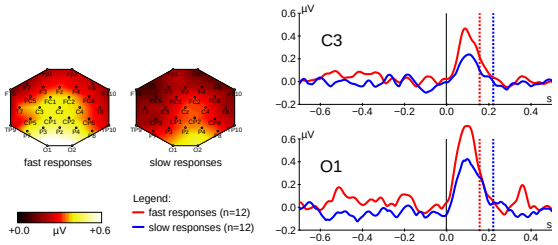

Figure 4.2.:
Evoked γ band responses for fast (red) and slow (blue) motor responses (right) and topographic maps of the evoked γ band responses in the time range 60 to 130 ms (left) averaged across all participants. The vertical black lines indicate stimulus onset, dotted lines indicate mean response times of fast response trials (red) and slow response trials (blue). Note the marked increase of the response for fast response trials.

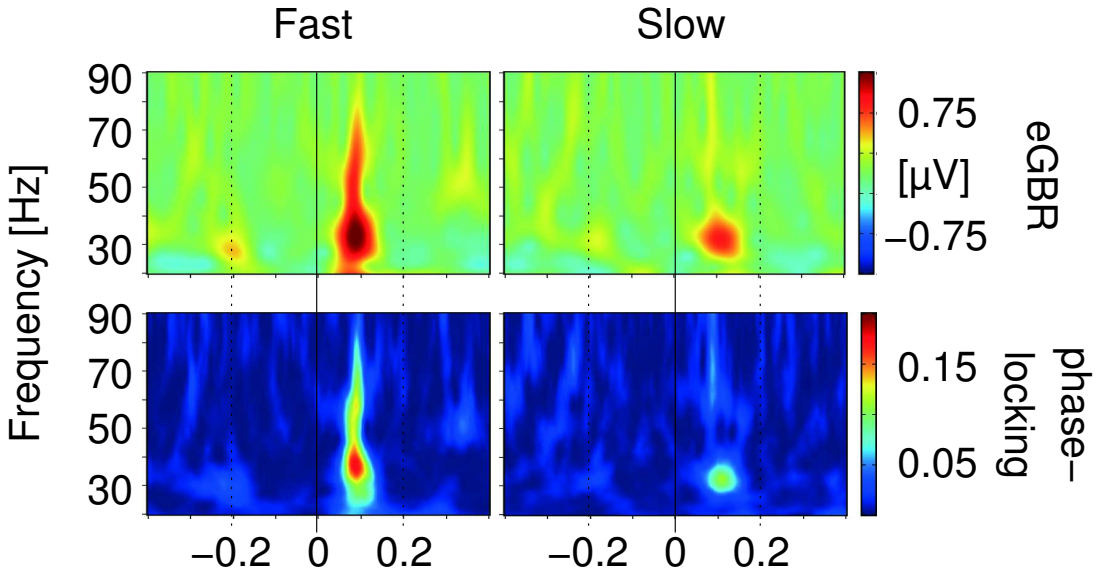

Figure 4.3.:
Time frequency representations of eGBR (top) and phase-locking factor (bottom) for fast responses (left) and slow responses (right) of a single representative participant. Bot measures show a considerable enhancement for fast responses.

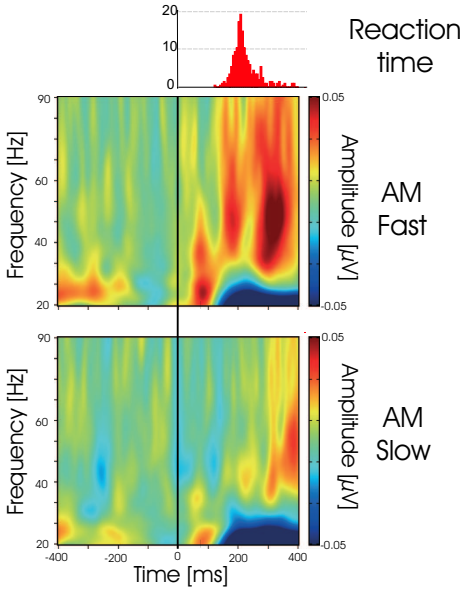

Figure 4.4.:
Total activity patterns for fast and slow motor responses and reaction time histogram. Top: reaction time histogram of all trials from all participants. Time axis is like below. Middle: Time frequency representation of total activity for fast response trials. Bottom: Time frequency representation of total activity in slow response trials. Data from the posterior ROI have been averaged to obtain the time frequency representations. Simulus onset is at 0 ms. Note that the response time histogram peaks considerably earlier than the total γ activity.

($F_{1,9} = 0.83$). In a later time window between 180 and 400 ms total activity was significantly modulated by response speed ($F_{1,9} = 8.51, p < 0.05$, Fig. 4.4). Note however, that this effect was found in most cases after the participants had already pressed the button.

4.3.4. Relation between stimulus preceding ERP and γ band response

In order to disentangle the relation between the slow negative potential and the eGBR, we split the trials into two groups of trials with either a pronounced prestimulus negativity (strong negativity trials) or a weak prestimulus negativity (weak negativity trials) and analyzed eGBRs separately in both subsets. No significant eGBR differences were found between trials with strong and weak negativity ($F_{1,9} = 0.96$). As depicted in Figure 4.5 on the next page, this was due to large standard deviations between single participants. Inspection of single participant data revealed that out of 11 participants, five demonstrated enhanced eGBRs in strong negativity trials compared to weak negativity trials, while two participants demonstrated decreased eGBRs in strong negativity trials compared to weak negativity trials. For the remaining four participants, eGBRs were virtually the same for strong negativity trials compared to weak negativity trials.

4.4. Discussion

In the current study we demonstrated that both ERPs and eGBRs are more pronounced for fast compared to slow responses. We further pointed out that the

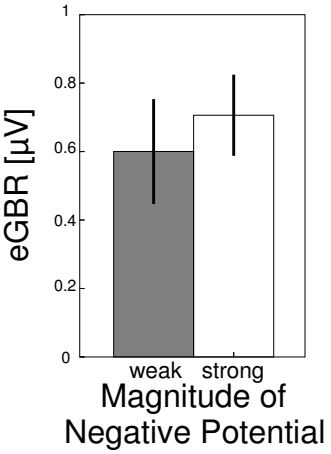

Figure 4.5.:
Strength of the eGBR in trials with weak and strong negative potential preceding the stimulus. Subaverages with weak prestimulus negative potential are marked in grey, subaverages with strong negative potential are marked in white. Error bars indicate standard error of mean. Note the large error bars, that result from the fact that less then half of the participants responded with an enhanced evoked γ peak in strong negativity trials, while this effect was even reversed in some participants.

enhanced eGBRs for fast responses are a result of increased phase-locking to the stimulus, rather than stimulus related amplitude modulations.

We observed a slowly increasing potential that appeared 500 ms before stimulus onset and was terminated by the participant's response. On the one hand, this negativity could reflect a contingent negative variation (CNV, Grey Walter, 1964). Such a CNV would be expected to vary between blocks depending on the degree of expectancy, i.e. the distribution of inter stimulus intervals (Trillenberg et al., 2000). However, in our paradigm no significant differences were found between the three blocks which differed in the distribution of inter stimulus intervals. On the other hand, the negativity might also reflect a readiness potential (Freude et al., 1989; Endo et al., 1999; Deecke et al., 1984). However, a readiness potential should normally be observed preceding self paced movements (Brunia, 1999), whereas in the current study no such movements were required. We demonstrated that this negative potential differed between fast and slow responses, which is in line with previous studies, that showed that reaction times are short if a pronounced readiness potential can be observed (Freude et al., 1989). Deecke et al. (1984) have argued that readiness potentials are recordable only before voluntary movements (actions) but not or to a lesser degree before reactions as in case of the reaction to a visual stimulus. In contrast, other authors also described readiness potentials before reactions to a stimulus (Endo et al., 1999; Leocani et al., 2001; Endl et al., 1999). Thus, based on our current data we cannot discriminate between a CNV and a readiness potential that preceds the stimulus. However, both types of slow potentials have been associated with anticipatory motor preparation (Brunia, 1999).

We could extend the ERP findings by showing a relation between evoked gamma oscillations and reaction time, indicating that fast reactions are associated with highly phase-locked γ oscillations. In line with the ERP results this effect was observed at central electrodes (Freude et al., 1989). However, in the current study we found significant differences between fast and slow response

trials also at posterior electrodes. Previous results indicating that eGBRs are highly dependend on physical factors of the stimulus, linked eGBRs to very early visual processing (Busch et al., 2004). This extends the findings obtained from ERP analysis by showing that fast and slow response trials differ already in earlier stages of visual processing. The current findings are in line with both findings from the auditory modality (Yordanova et al., 2001; Jokeit & Makeig, 1994) as well as models that link rapid feedforward processing of spike timings with phase-locked gamma oscillations (Körner et al., 1999). Furthermore, GBRs seem to be facilitated when participants are required to make a behavioral response compared to when no responses are required (De Pascalis & Ray, 1998).

It might be argued that the observed effects are, although triggered by the stimulus, mainly a manifestation of anticipation of the stimulus. Such an effect should take place already before the stimulus would be applied. It has been reported that such anticipation effects vary with the randomization procedure used for inter stimulus intervals (Trillenberg et al., 2000). Although different randomization procedures were used for the different blocks of the experiment, no effect of the randomization procedure was observed. This favors the interpretation that the electrophysiological effects are related to facilitation of stimulus processing rather than anticipation of stimulus timing in fast response trials.

Due to its similar frequency characteristics, electromyographic activity is usually a big problem when dealing with EEG γ activity (cf. Chapter 2). We visually inspected every trial before analysis to make sure that there was no excessive high frequency activity in the data. Still there might be muscular activity in the data, with an amplitude that is too low to be detected visually. However, the γ activity in the present study displays one important property that cannot be expected for such low amplitude muscular activity: it is phase-locked to a visual stimulus while showing virtually no power increase. Furthermore, low amplitude muscular activity would be expected to have a constant tonus which would be subtracted with the baseline. Therefore, we believe that the results described here can be related to cerebral processing rather than muscular artifacts.

How do the slow negative potential and the findings about phase-locked gamma oscillations fit together? While slow negative potentials like CNV or readiness potential are usually associated with anticipatory motor activity (for review see Brunia, 1999), eGBRs have been linked to early visual processing (Busch et al., 2004). These two phenomena might be related in two different ways: First, the slow negativity might be a prerequisite for an enhanced eGBR, which in turn enables the participant to perform a rapid response. Second, the slow negativity as well as the eGBR might independently facilitate rapid reactions. The fact, that we did not find significant differences in eGBR for different magnitudes of the slow negativity in single trials, is in line with the second alternative. However, further research in this direction is needed to reveal the exact relations between these two brain signals and behavioral performance. In such an experiment the stimulus preceding ERP and poststimulus γ band activity could be dissociated

by experimentally suppressing one of these phenomena independently by an appropriate experimental manipulation.

We observed very fast reaction times in the current study. Compared to the reaction times of 400-600 ms (e.g. Schmiedt et al., 2005; Busch et al., 2004) observed in simple cognitive experiments, 200 ms might seem very short. It should be kept in mind, that in the current experiment no stimulus discrimination was necessary. Taking into account the high contrast and very low spatial frequency (one big square, no texture) of the stimuli used in the present study, reaction times around 200 ms fit well with the expected reaction times as estimated by Plainis & Murray (2000).

Previous studies reported correlations of either γ peak latency (Haig et al., 1999) or amplitude (Jokeit & Makeig, 1994) with reaction time. However, in both studies effects were observed after the participant's average response time. Furthermore, these studies did not analyze phase-locking of the activity. Although our data also include late, stimulus induced amplitude modulations, which also vary with reaction time, we show that fast and slow response trials differ with respect to their phase-locking even before amplitude modulations start to play a role. Furthermore, the fact that the effect on total γ activity only becomes significant after the participants already have responded, excludes the latter from being a causal factor determining the reaction time differences. These results might indicate that phase-locked GBRs play an important role in fast detection of visual stimuli, whereas induced GBRs might be linked to further refinement of this initial classification, as has been suggested by recent models of visual processing (Körner et al., 1999; Herrmann et al., 2004).

The current results demonstrate that rapid visual processing in preparation for a speeded response is (at least partly) dependent on stimulus locked activity in the γ range. However, the actual behavior in a cognitive task is most probably based on the interactions of different oscillatory processes. Indeed, movement seems to be related to other, probably lower frequencies (Neuper & Pfurtscheller, 2001). Also the integration of different modalities to a coherent movement has been associated with oscillatory activity at lower frequencies (Pineda, 2005). In contrast, the observed effects in the γ range seem primarily related to visual processing, albeit preparing the brain for speeded responses. It has been argued recently that high frequency oscillations which are evoked in early sensory areas need to be down-modulated to lower frequencies that then cover more distributed areas of the brain (Chen & Herrmann, 2001; Olufsen et al., 2003). Thus, it seems plausible to assume that early evoked γ activity might be necessary but not sufficient for speeded responses. Later activity of lower frequency seems to relay the results of the enhanced visual processing to motor areas. Indeed, lower frequencies during a visual motor integration task have been reported to be highly synchronized between visual and motor areas in cats (Roelfsema et al., 1997).

In conclusion we could show that fast reaction times are associated with enhanced phase-locking in the γ range. Evoked γ activity might thus be related to

a fast mode of visual processing.

5. Experiment III: Effects on γ band activity depend on time constraints of the behavioral task

The experiment described in this chapter have been published in the Journal "PLoS one" (Fründ et al., 2008).

5.1. Introduction

In everyday life, actions need to be continuously adjusted to sensory input. This requires fast processing of sensory stimuli in order to make them available for motor reactions. At the same time, there are numerous situations in which more detailed analyses are required to refine the perceptual outcome and adapt future behavior (Rodemann & Körner, 2001). Are these functions governed by the same neural system or do we use different systems for these tasks? Which physiological processes might mediate these functions?

Speed of processing could be achieved by rapid feedforward categorization of incoming stimuli (Körner et al., 1999; Thorpe et al., 2001, see also Chapter 1). More detailed analyses seem to rely on feedback to refine these initial categories (Hochstein & Ahissar, 2002; Körner et al., 1999; Lamme & Roelfsema, 2000). Recently Herrmann et al. (2004) linked these two modes of processing to different aspects of EEG γ band oscillations. Rapid stimulus categorization seems to be accompanied by early phase-locked, so called evoked γ band responses (eGBRs, latency approximately 100 ms, gamma band: 30-90 Hz, see also Chapter 4). Later refinement of these quickly established categories has been linked to late induced γ band responses (iGBRs, latency approximately 300 ms). We know that the response characteristics of evoked and induced GBRs differ considerably with respect to several aspects of processing. Evoked GBRs are highly dependent on the physical salience of the stimulus (Busch et al., 2004). Although it has been argued that they were mainly a sensory phenomenon (Karakaş & Başar, 1998), other reports point out that eGBRs are modulated by attention (Busch et al., 2006; Tiitinen et al., 1993; Yordanova et al., 2001). Recent reports also suggest a link between eGBRs and matches between incoming sensory information and experience based object templates (Herrmann et al., 2004; Morup et al., 2006). If a stimulus matches with such an object template, this was assumed to result

in increased firing. The consequences of such a match are twofold; (i) information is more efficiently relayed to later stages of processing, (ii) feedback signals from the locus of the match are enhanced. Herrmann et al. (2004) argued that especially these feedback signals could result in activity reverberating between low level visual areas at γ frequencies. In contrast, iGBRs seem to be related to the semantic content of the stimuli (Busch et al., 2006; Gruber & Müller, 2005; Tallon-Baudry et al., 1998). If a semantic representation is generated during multiple presentations for a particular class of stimuli, this also leads to the emergence of increasingly strong iGBRs (Gruber & Müller, 2005). Evoked and induced GBRs also differ with respect to their dynamic properties. While eGBRs seem to be mainly a phenomenon of increased phase-locking to the stimulus (Busch et al., 2006; Fründ et al., 2007), iGBRs occur as amplitude increases with varying latency after the stimulus (Basar-Eroglu et al., 1996; Tallon-Baudry & Bertrand, 1999). Since timing as manifested in phase-locking to the stimulus is the first available information about a stimulus (Cariani, 2004), a fast processing mechanism should employ timing information to discriminate different stimuli (Thorpe et al., 2001). In conclusion, these findings are in line with the idea that eGBRs are related to fast processing of upstream information, whereas iGBRs are related to more elaborated processing based on the integration of upstream and downstream information (Körner et al., 1999).

In this third experiment, we want to test the idea that (i) eGBRs are related to rapid initial processing and (ii) that iGBRs are related to the subsequent refinement of the stimulus representation. If the functional relevance of eGBRs is a rapid discrimination of stimuli, differences in eGBR between meaningful and meaningless patterns should be particularly salient in a speeded response task that can only be based on rapid stimulus discrimination. We expected that a further refinement of the initial rough categorization would only be possible for more complex stimuli. If such refinement processes were related to iGBRs, differences in iGBR between meaningful and meaningless stimuli should be more pronounced with the more complex stimuli. Participants were required to categorize objects and object-like but meaningless patterns (non-objects) as meaningful and meaningless. In the speeded response condition they were required to select the correct button as fast as possible, whereas in the delayed response task, no time pressure was imposed. These two tasks were performed on two different sets of stimuli. One set of stimuli contained black and white line drawings of objects and non-objects (stimulus Set A, see left column of Figure 5.1). Another set of stimuli contained more natural, colored pictures of objects and non-objects (stimulus Set B, see right column of Figure 5.1).

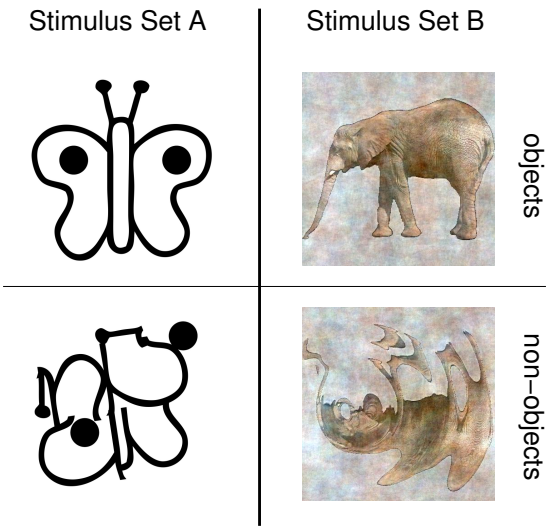

Figure 5.1.:
Example stimuli employed in the current experiment. Left column: an example of an object and a non-object stimulus from stimulus Set A. Right column: an example of an object and a non-object stimulus from stimulus Set B is shown.

5.2. Methods

5.2.1. Participants

Seventeen healthy participants (mean age: 23.76±2.34 years, range: 20 to 28 years, 5 m, 12 f) participated in the current study. Participants did not report any current or past psychiatric or neurological disorders and received money or course credits for their participation. The experimental procedure was in accordance with the Declaration of Helsinki as well as with the guidelines of the local ethics committee of the Otto-von-Guericke University of Magdeburg.

5.2.2. Stimuli and experimental procedure

During the experiment participants observed stimuli from two different sets of stimuli. Both these sets encompassed pictures of semantically meaningful objects and object-like patterns that did not correspond to a particular semantic content. One set of stimuli consisted of schematic line drawings (Set A). The other set of stimuli consisted of images that were colored and had a broad band spectrum of spatial frequencies (Set B).

Stimuli in Set A were all high contrast schematic black on white drawings. Non-objects were constructed by rearranging the lines from the objects. This way, the number of black and white pixels and the number of black and white edges was approximately the same for object and non-object stimuli. A detailed description of the stimuli in Set A can be found elsewhere (Herrmann et al., 2004). Examples for stimuli from stimulus Set A are shown on the left side of Figure 5.1. Stimuli in Set B were derived from images of natural objects. To obtain a set of non-object stimuli, these images were distorted. From this set of original and distorted images, stimulus Set B was derived by averaging the amplitude spectra

of spatial frequencies and differentiating the stimuli only by means of their phase spectra. A detailed description of the stimuli in Set B can be found elsewhere (Busch et al., 2006). Examples for stimuli from stimulus Set B are shown in the right column of Figure 5.1.

Each set of stimuli was presented in two blocks of 200 stimuli each (100 objects and 100 non-objects). Participants were instructed to press a button with one hand to indicate that the current stimulus represented a meaningful object and to press another button with the other hand to indicate that the current stimulus represented a meaningless non-object. In one of the two blocks, participants were to press the button as quickly as possible (speeded response). In the other block, they were to press the button one second after the onset of the stimulus, after a response screen had been presented (delayed response). Thus, each participant responded to a total of four blocks: one block with stimuli from Set A and speeded response requirements, one block with stimuli from Set A and delayed response requirements, one block with stimuli from Set B and speeded response requirements and one block with stimuli from Set B and delayed response requirements. Each block was preceded by a practice block of 16 trials that was not analyzed. During the practice block participants were able to become familiar with the stimuli and the task demands of the new block. Block sequence and response buttons were counterbalanced across participants.

Stimuli were presented on a 24" TFT-display at a distance of 122 cm. The stimuli subtended a region of ≈ 8 to 10 degree visual angle which has been shown to be suitable to evoke GBRs (Busch et al., 2004; Fründ et al., 2007). The stimuli were presented in randomized order with interstimulus intervals drawn from a uniform distribution between 1000 and 2000 ms. Stimulus duration was 1000 ms in the speeded response task and 500 ms in the delayed response task. In the delayed response blocks, there was a 500 ms delay after each stimulus before the response screen was presented. This way, block duration was kept approximately constant in order to avoid fatigue effects. Participants were instructed to fixate a small black cross that was presented at the center of the presentation screen.

5.2.3. Data acquisition

Participants performed the experiment in an electrically shielded, sound-attenuated, and dimly lit cabin (IAC, Niederkrüchten, Germany). The stimulation monitor was placed outside the cabin behind an electrically shielded window. All devices inside the cabin were battery operated to avoid line frequency interference (50 Hz in Germany). The electroencephalogram (EEG) was measured from 31 scalp locations according to an extended 10-20 system. The nose served as reference. In order to detect artifacts due to eye movements, an electrode placed below the orbital rim recorded the electrooculogram (EOG). Activity was recorded using sintered Ag/AgCl electrodes mounted in an elastic cap (Easycap, Falk Minow, Munich, Germany). Electrode impedances were kept below 5 kΩ. The EEG

was filtered between 0.02-250 Hz, digitized at a rate of 500 Hz, and stored on a computer hard disk for off-line analysis. A fiber optic cable transferred the digitized EEG to a computer outside of the recording cabin. A digital high pass filter with a cutoff frequency of 0.5 Hz was applied offline in order to avoid slow shifts in the baseline. If participants moved their eyes away from the fixation cross, it was detected by measurements of EOG activity and the trial was discarded. For this purpose, an automatic artifact detection was computed, which excluded trials from further analysis if the standard deviation within a moving 200 ms window exceeded 40 μV in one channel. The automatic artifact rejection was supplemented by visual inspection of every trial to ensure that only trials without artifacts were included in the subsequent analysis.

5.2.4. Data analysis

For all trials, the percentage of correct responses was ascertained. In addition, mean reaction times were determined for speeded response trials with respect to stimulus onset. Mean reaction times were determined for delayed response trials with respect to the onset of the response display (1000 ms after stimulus onset).

Event related potentials (ERPs) were computed as averages of all artifact-free trials of a given condition. These curves were aligned by subtracting baseline activity from the last 200 ms preceding stimulus onset. Grand average time courses were computed by averaging ERP waveforms from all participants.

Gamma band responses were characterized by three parameters derived from the EEG by means of the wavelet transform (Morlet wavelet with 12 cycles, time frequency localization at 40 Hz: $2\sigma_t \approx 50$ ms, $2\sigma_f \approx 13$ Hz). (i) The evoked activity, which is the amplitude of the wavelet transform of the ERP; (ii) the total activity, which is the averaged absolute amplitude of the single trial wavelet transforms; and (iii) the degree of phase-locking (PL) to the stimulus, quantified by the phase locking factor from Chapter 2 Equation (2.12) on page 22. It has been demonstrated that the exact frequency of the GBR varies in a very consistent manner across participants (Fründ et al., 2007). To account for frequency variations across participants, the time frequency planes from each participant were averaged across all conditions. The response frequency was defined as the frequency that displayed the strongest deviation from a baseline (200 to 100 ms before stimulus onset). Two different response frequencies were ascertained: the frequency of the eGBR, as local maximum of evoked activity in the time range between 60 and 140 ms after stimulus onset and the frequency of the iGBR as local maximum of total activity in the time range between 200 and 400 ms after stimulus onset. In both cases, response frequencies were determined from the frequency range between 30 and 90 Hz. Response frequencies of the eGBR were between 32 and 66 Hz (mean 42 Hz) and response frequencies for iGBR were between 35 and 69 Hz (mean 50 Hz). Time courses of evoked and total activity as well as PL were extracted at these two frequencies.

To avoid loss of statistical power, electrodes were pooled into regions of interest (ROI). Responses were evaluated from a posterior ROI (electrodes O1, O2, P7, P3, Pz, P4 and P8) and from a central ROI (electrodes CP1, CP2, C3, Cz, C4, FC1, FC2). These ROIs were chosen from those electrodes, that displayed a strong signal change after stimulation. Repeated measurements analyses of variance were used to judge statistical significance of the factors TIME PRESSURE (speeded vs. delayed response), OBJECTNESS (object vs. non-object), STIMULUS COMPLEXITY (schematic line drawings from Set A vs. natural images from Set B) and ROI. Separate analyses of variance were performed on the percentage of correct responses (without the factor ROI), on mean ERP amplitude between 250 and 400 ms, and on early (mean amplitude between 60 and 140 ms) and late (mean amplitude between 200 and 400 ms) GBR.

5.3. Results

5.3.1. Behavioral data

Mean reaction times were generally faster for the more detailed stimuli from Set B than for the line drawings from stimulus Set A ($F_{1,16} = 21.03$, $p < 0.001$). In addition, mean reaction times in the delayed condition (response time relative to the response screen one second after stimulus onset) were on average 178 ms shorter than in the speeded response condition (response time relative to stimulus onset, $F_{1,16} = 322.87$, $p < 10^{-11}$). In the speeded response task, participants made significantly more errors compared to the delayed response task ($F_{1,16} = 34.63$, $p < 10^{-4}$). Participants also made more errors with line drawings from stimulus Set A than with colored stimuli from stimulus Set B ($F_{1,16} = 23.06$, $p < 0.001$). This was particularly true in the delayed response task (STIMULUS COMPLEXITY $\times$ TIME PRESSURE interaction: $F_{1,16} = 12.14$, $p < 0.01$). See Figure 5.2 for a summary of the behavioral results.

5.3.2. Event related potentials

A late modulation of the event related potential (ERP) was observed between 250 and 400 ms (see Figure 5.3). The most prominent effect in this time window was a strong modulation of the average amplitude in the time range 250 to 400 ms when the stimuli were objects ($F_{1,16} = 151.27$, $p < 10^{-8}$).

5.3.3. Early γ band response

Figure 5.4 displays time frequency representations of evoked oscillatory activity in a single participant (top) and averages across all participants (middle). A clear eGBR can be observed for the single participant which is smeared in the averaged

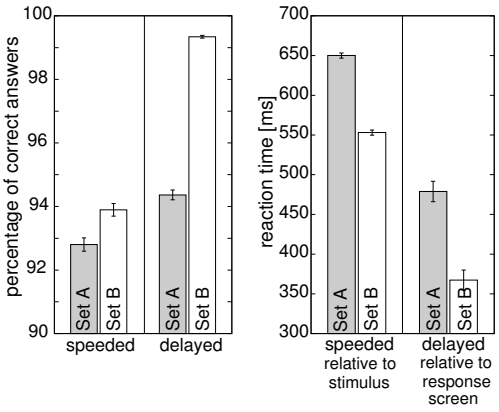

Figure 5.2.:
Behavioral data in the current experiment. Left display: percentages of correct responses. Right display: reaction times. Results from schematic line drawings (Set A) are marked in grey. Results from colored, more complex images (Set B) are marked in white. Note that the accuracy benefit from the additional information contained in stimuli from Set B is much more pronounced for delayed responses. Note also that reaction times in the speeded task refer to stimulus onset, while in the delayed task reaction times refer to the onset of the response screen which appeared 1000 ms after stimulus onset.

activity due to considerable variance in the response frequencies between subjects. In order to perform statistical analyses of this activity, time courses at the peak frequency of the response were selected for further analysis.

These evoked GBRs are depicted in Figure 5.5. An eGBR could be observed in all participants. The eGBR differed between object and non-object stimuli only if a speeded response was required (TIME PRESSURE × OBJECTNESS interaction: $F_{1,16} = 5.00$, $p < 0.05$). To differentiate between stimulus related changes in oscillatory amplitude and oscillatory phase, we calculated the average analytic amplitude across all trials (total oscillatory activity) and the phase locking factor (Tallon-Baudry et al., 1996b). The effect on eGBR was not accompanied by any recognition related effect of total oscillatory activity (no significant effect in ANOVA, see Figure 5.7, although this displays results with frequencies adapted to the late response). Similar to evoked activity, phase locking of the early GBR to the stimulus differentiated object and non-object stimuli in the speeded response task (TIME PRESSURE × OBJECTNESS interaction: $F_{1,16} = 5.08$, $p < 0.05$, see Figure 5.6). Phase locking was also significantly enhanced at posterior electrodes (main effect of ROI: $F_{1,16} = 33.08$, $p < 10^{-4}$) and for stimulus Set A (main effect of STIMULUS COMPLEXITY: $F_{1,16} = 7.50$, $p < 0.05$). In Figure 5.5 there seems to be a difference in prestimulus activity between object and non-object stimuli for stimulus Set B in the speeded response task. However, this difference was not statistically significant ($t_{16} < 1.24$, $p > 0.2$).

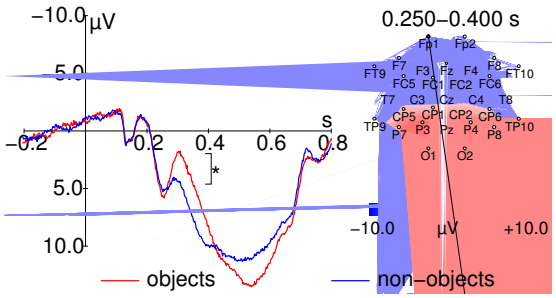

Figure 5.3.:
Event related potentials. Left: ERP-waveform at Pz for object (red) and non-object (blue) stimuli. Right: topographic map of averaged activity from all conditions between 250 and 400 ms after stimulus onset. Note that the clear late negative deflection is observed for object stimuli only. The asterisk indicates a significant difference that is described in the text.

5.3.4. Late γ band response

At the bottom of Figure 5.4, a late enhancement of total gamma band activity can be observed. The late γ band response was also characterized by a clear peak in the time courses of total γ activity (see Figure 5.7). This peak had a very broad spatial distribution and was more pronounced for schematic line drawings from stimulus Set A (main effect STIMULUS COMPLEXITY: $F_{1,16} = 4.80$, $p < 0.05$). However, recognition related modulations of late total γ activity were only observed for the more natural images from stimulus Set B (STIMULUS COMPLEXITY $\times$ OBJECTNESS interaction: $F_{1,16} = 5.11$, $p < 0.05$).

5.4. Discussion

In the current report, we investigated how different types of γ band responses (GBRs) can be modulated depending on task requirements and stimulus complexity. Early evoked GBRs differentiated between objects and non-objects, irrespective of stimulus complexity, only when participants had to perform speeded discriminations. Later induced GBRs differentiated between objects and non-objects irrespective of response demands, only for complex stimulus material.

Previous studies related eGBRs to a fast processing mode based on temporal information (Körner et al., 1999, see also Chapter 4) which allows stimulus classifications within 100-150 ms after stimulus onset (Thorpe et al., 1996). The current results confirm this hypothesis. Early differences between meaningful and meaningless stimuli become manifest in the temporal structure, i.e. the phase-locking of the eGBRs. The results also indicate that this fast mode seems to be used predominantly in those cases in which a speeded response was required. In situations that do not require a speeded response, additional information from a refinement system (presumable expressed in the induced GBR) can further shape the response. The error rates in the current experiment are in line with

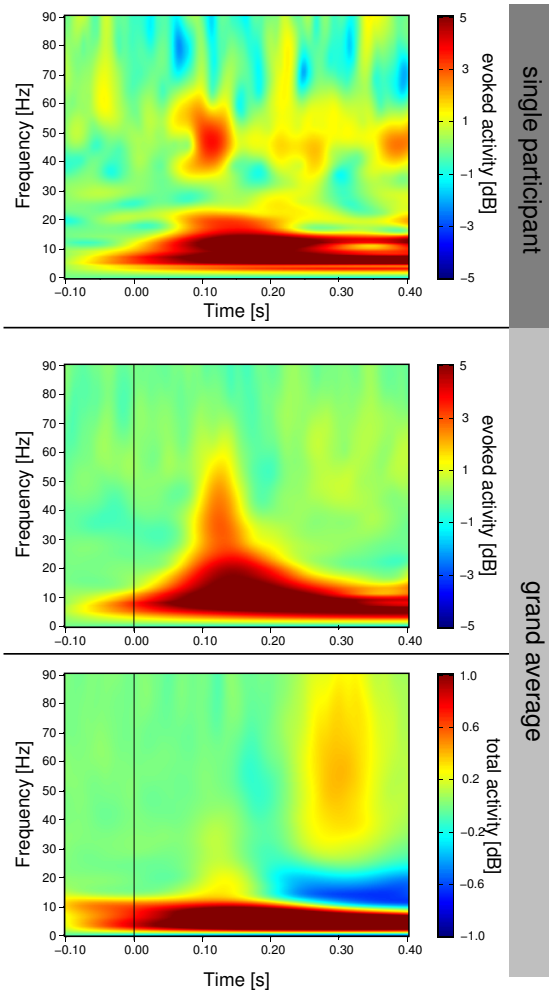

Figure 5.4.:
Time frequency representations of oscillatory activity. Top: evoked activity from a single representative participant. Middle: evoked activity averaged across all participants. Bottom: total activity averaged across all participants. Note how averaging smeares the relatively focal activity of single participants. These data have been obtained by averaging time frequency planes from the posterior ROI.

this interpretation. Although a difference in the physiological response can be observed, the additional information contained in the more natural stimuli cannot completely be utilized in the speeded response task.

Reactions to the more natural stimuli were generally faster than those to the line drawings in line with previous results (Rossion & Pourtois, 2004). This might indicate that participants benefit from the additional information contained in the natural stimuli. In the speeded response condition, participants had to first perceive the stimulus and use this information to immediately initiate a response. In contrast, in the delayed condition, participants could perceive the stimulus and prepare their response before the response screen appeared. If we assume that response execution takes approximately the same time in the speeded task and in the delayed task, the difference in reaction time gives a coarse estimate of the time required to identify the stimulus in the speeded response task. This time, which is ≈ 180 ms, is clearly below the latency of the late γ band response, yet still includes the early gamma band response. Thus, we infer that responses in the speeded response condition are based on the evoked GBR, whereas responses

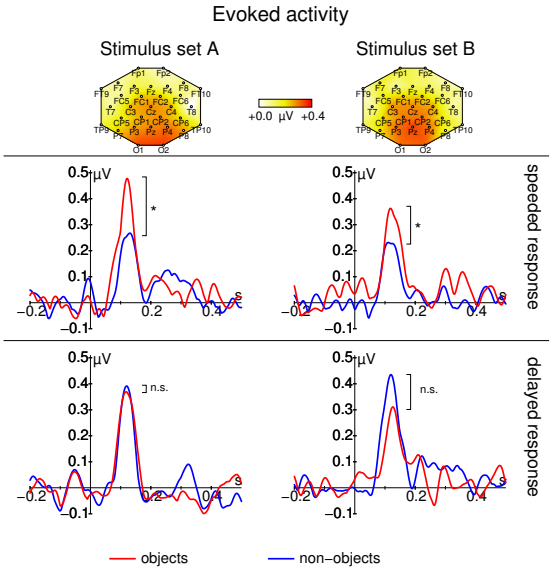

Figure 5.5.:
Early evoked γ band response to object (red) and non-object (blue) stimuli. Data from stimulus Set A (schematic black and white line drawings) are shown in the left column; data from stimulus Set B (natural colored images) are shown in the right column. The top row shows topographic maps of the averaged activity from all conditions between 60 and 140 ms. In the second row, eGBRs for the speeded response task are shown. In the third row, eGBRs for the delayed response task are shown. All time course data are taken from Pz. Note that eGBRs to object stimuli are enhanced only if participants need to perform a speeded response. Response frequencies have been determined from the time range 60-140 ms. Asterisks mark significant differences that are described in the text, n.s. denotes nonsignificant differences.

in the delayed response condition, might be initiated only after information from both, early evoked and late total GBR has been integrated. Participants seemed to benefit from this additional information only for the more natural stimuli.

The late γ band amplitude modulation is comparable with respect to latency, frequency and recognition modulation to what other authors have termed induced GBR (Gruber & Müller, 2005; Busch et al., 2006; Tallon-Baudry et al., 1998). This seems to indicate that iGBRs only discriminate semantically meaningful objects from object-like but meaningless patterns if the stimuli provide a sufficient amount of detail. Interestingly, iGBRs have also been related to learning new stimuli (Gruber & Müller, 2006; Axmacher et al., 2006). This is in line with the interpretation that iGBRs relate to a refinement system (Körner et al., 1999), the output of which could be used to modify future behavior (Rodemann & Körner, 2001). Here, we propose that this refinement system is only activated if the stimuli are sufficiently complex to support a further refinement. An example for stimuli that are not sufficiently complex for further refinement seems to be given by the schematic line drawings.

Figure 5.6.:
Phase locking (PL) of the early γ band response to object (red) and non-object (blue) stimuli. Data from stimulus Set A (schematic black and white line drawings) are shown in the left column. Data from stimulus Set B (natural colored images) are shown in the right column. The top row shows topographic maps of the averaged phase locking from all conditions between 60 and 140 ms. In the second row, PL for the speeded response task is shown. In the third row, PL for the delayed response task is shown. All time course data are taken from Pz. Note that PL after presentation of object stimuli is enhanced only if participants need to perform a speeded response. Response frequencies have been determined from the time range 60 to 140 ms after stimulus onset. Asterisks mark significant differences that are described in the text, n.s. denotes nonsignificant differences.

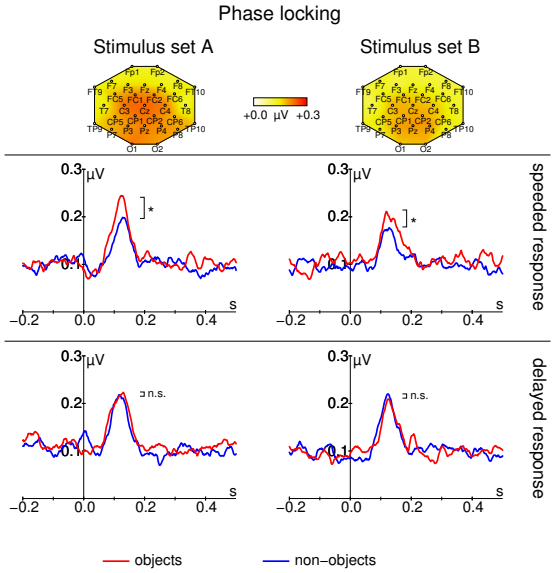

In the speeded response condition, participants seemed to base their responses on coarse and global categorizations of the stimulus. This might indicate that the initiation of a button press can be based on such global categorizations even before all the details of a stimulus have been processed. A similar account comes from the reverse hierarchy theory (Ahissar & Hochstein, 2004; Hochstein & Ahissar, 2002). This theory states that incoming stimuli are rapidly relayed to higher visual areas. Conscious access to incoming stimuli then proceeds from global categorizations to successive levels of detail. The current findings link these two processing modes within the same system to evoked and induced GBRs (Körner et al., 1999; Herrmann et al., 2004). In an initial, fast but coarse, classification step, information is rapidly relayed to higher perceptual areas. This classification depends on the temporal fine structure of the spike wave triggered by the stimulus (Körner et al., 1999). It has been suggested that such rapid processing could be mediated by the dorsal visual pathway (Bar, 2003; Bar et al., 2006). Different authors emphasized that initial, fast but coarse classifications should be based on

feedforward processing (Lamme & Roelfsema, 2000; Hochstein & Ahissar, 2002). From a modeling study, Rodemann & Körner (2003) inferred that the reliability of classifications by such a system strongly depends on the presence of evoked γ oscillations. After this initial classification, feedback connections ensure that the information reverberates within the visual system (Körner et al., 1999; Lamme & Roelfsema, 2000). This leads to a refinement of the percept (Rodemann & Körner, 2001) and induced γ band oscillations (Körner et al., 1999; Engel et al., 2001; Fründ & Herrmann, 2007). These oscillations could, in turn, be used to adapt future behavior based on learning (Axmacher et al., 2006; Körding & König, 2000). The current findings demonstrate that these two modes can be modulated separately by fairly general experimental manipulations.

Previous reports that investigated recognition related GBRs either found effects on evoked (Herrmann et al., 2004; Morup et al., 2006) or on induced GBRs (Gruber & Müller, 2005; Busch et al., 2006), but not on both at the same time. The current results resolve this issue. The stimuli used by those authors that reported effects on eGBRs (Herrmann et al., 2004; Morup et al., 2006), were probably too simple to elicit significant effects on later iGBRs. Note that these stimuli are the same as those used in the present report in stimulus Set A. There seem to be different reasons why authors found recognition effects on iGBRs but not on eGBRs. Busch et al. (2006) employed the same stimuli that we used in stimulus Set B in a delayed response task and reported effects on iGBRs, but not on eGBRs. It seems that the absence of a recognition effect on eGBRs in their data can be explained by the lack of time pressure in their experiment. In the experiment by Gruber & Müller (2005), no response delay was imposed. However, in this experiment, stimuli were reported to be relatively small ($\approx 4.5 \times 5.2°$). Recent findings suggest that eGBRs are highly dependent on stimulus parameters, in particular size (Busch et al., 2004; Fründ et al., 2007). Furthermore, the size of a stimulus not only seems to be a prerequisite for reliably measuring eGBRs but also for detecting top-down effects on eGBRs (Busch et al., 2006). Thus, it might be expected, that the stimuli employed by Gruber & Müller (2005) were not large enough to evoke a detectable GBR effect.

In conclusion, we were able to demonstrate that two different visual processing modes can be discriminated. One of these streams mediates rapid, but less accurate, categorization processes and seems to be based mainly on temporal relations to the stimulus as quantified by evoked γ band responses. The other stream is slower, but more accurate, and seems to be based on temporal relations between neural groups as quantified by induced γ band responses.

Figure 5.7.:
Total γ band activity after presentation of object (red) and non-object (blue) stimuli. Data from stimulus Set A (schematic black and white line drawings) are shown in the left column. Data from stimulus Set B (natural colored images) are shown in the right column. The top row displays topographic maps of the averaged activity from all conditions between 200 and 400 ms. In the second row, total γ band activity in the speeded response task is shown. In the third row, total γ band activity in the delayed response task is shown. All time course data are taken from Pz. Note that total γ band activity responds in a highly stimulus specific way: Although strongest responses are observed for stimulus Set A, differences between object and non-object stimuli can only be found for the more natural stimuli in stimulus Set B. Also note that there is no early response at all. Response frequencies have been determined from the time range 200 to 400 ms after stimulus onset. Asterisks mark significant differences that are described in the text; n.s. denotes nonsignificant differences.

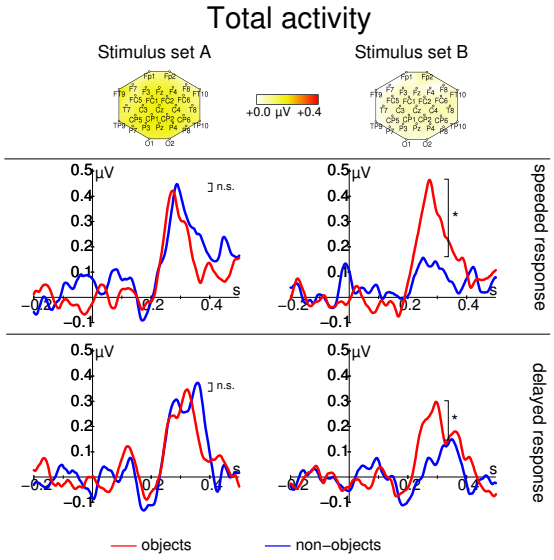

6. General Discussion

In Chapters 3, 4 and 5, we presented data, that indicated a relation between evoked γ band responses and rapid motor reactions. Based on the considerations from Chapter 1, these data are in line with the interpretation of oscillatory γ activity as a control signal for rapid neural information processing. However, some questions remain. In the following sections we will address some of these points. Although in most cases there are no conclusive answers, we believe that there are at least data that render some interpretations more plausible than others.

6.1. The origin of evoked γ oscillations

Where do evoked γ band responses come from? Which neural structures are involved in their generation? How do different neural mechanisms interact, to establish a temporally stable framework that reveals itself on the scalp in the form of evoked γ band responses? The data reviewed in this section are meant to give a rough idea of the origins of γ band activity in general and particularly evoked γ band responses. However, this review is not meant to be exhaustive. Recent reviews about these topics can be found elsewhere (e.g. Traub et al., 1998; Whittington et al., 2000 for cellular mechanisms and Singer & Gray, 1995; Engel et al., 2001; Llinás et al., 1998; Herrmann et al., 2004 for large scale oscillations).

6.1.1. Cellular origins of γ oscillations

In a series of studies, Traub et al. (1998) and Whittington et al. (2000) demonstrated that networks that include mutually interconnected inhibitory interneurons synchronize at high frequencies, mainly in the γ range. They studied two extreme cases that are replicated in Figure 6.1. If a network that does only include inhibitory connections is exposed to a tonic depolarizing current, the cells synchronize at a frequency in the γ range (see Figure 6.1, (b)). This cannot be observed if there are no connections at all as in Figure 6.1 (a). The extreme case of γ oscillations in purely inhibitory networks was termed interneural network γ (ING, e.g. Traub et al., 1998). In Figure 6.1 (c) a network is depicted that includes both, excitatory and inhibitory cells. If the excitatory neurons are strongly depolarized (e.g. by tetanic stimulation), they drive the inhibitory cells and the network synchronizes at a frequency in the γ range (Whittington et al., 2000).

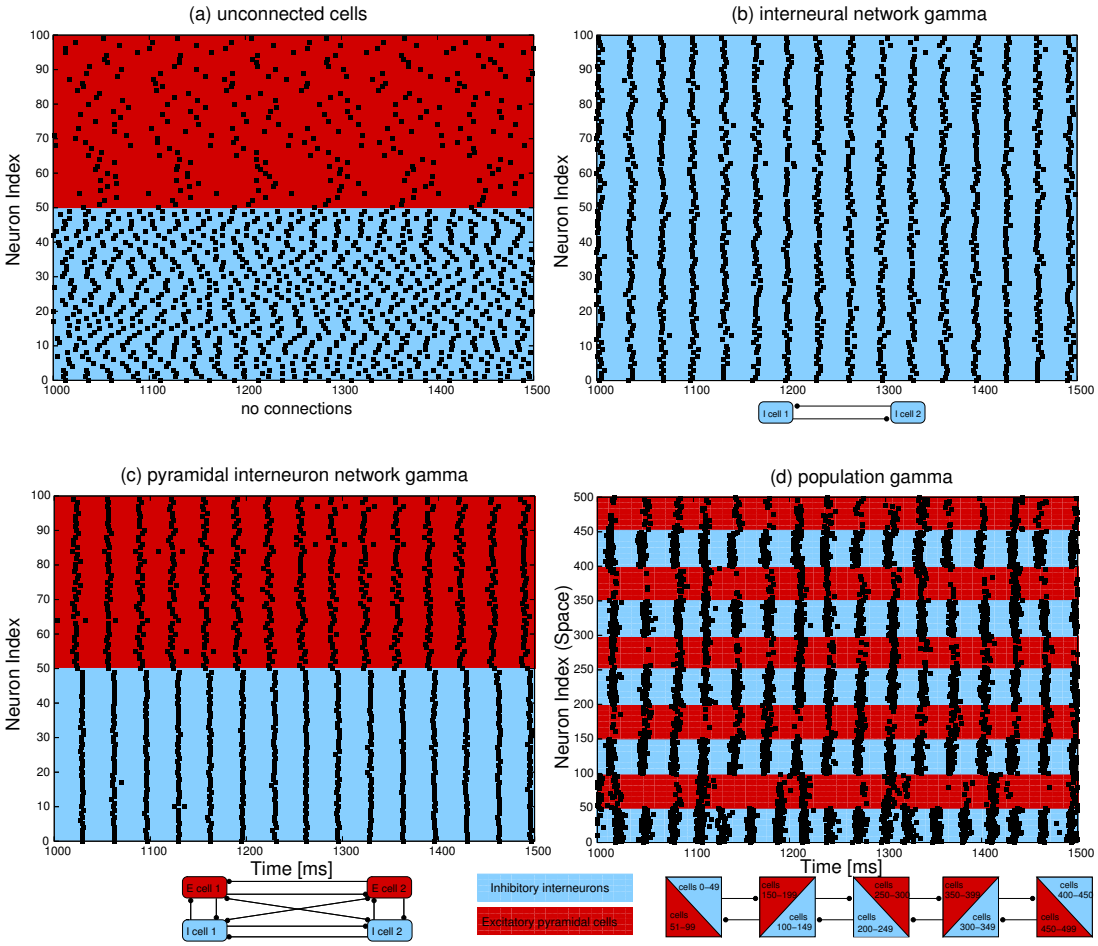

Figure 6.1.:
Different cellular origins of network γ oscillations. Spike rastergrams and sketches of the network connectivity for computational models of (a) fifty pyramidal cells and fifty interneurons without mutual connections (b) one hundred mutually connected interneurons generating interneural network γ (c) fifty pyramidal cells and fifty interneurons with mutual connections generating pyramidal interneuron network γ (d) 500 cells organized in five pools of fifty pyramidal cells and fifty interneurons each. Neighbouring pools are mutually connected. Note that in this case excitatory pyramidal cells do not fire at all cycles but still make up a γ oscillation in the summed activity. Spike rastergrams have the time on the x-axis and the index of the neuron on the y-axis. If a particular cells fires a spike, a small black square is drawn at that position. All cells have been modeled using the generalized integrate and fire neuron proposed by Izhikevich (2003).

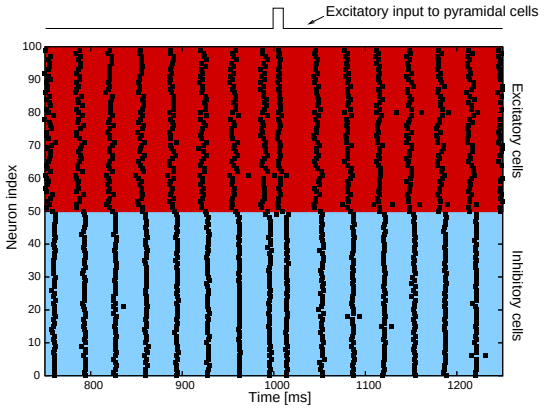

Figure 6.2.:
Raster plot showing a phase reset induced by a brief, strong excitatory pulse applied to the excitatory pyramidal cells in a PING network. Pyramidal (excitatory) cells are marked in red, (inhibitory) interneurons are marked in blue. Although a marked change in the firing dynamics can be observed around the time of the pulse, only a weak change of the phase of the ongoing oscillation is induced.

This extreme case of γ oscillations were the inhibitory cells are driven by the excitatory pyramidal neurons is termed pyramidal interneuron network γ (PING, e.g. Traub et al., 1998). In normal neural tissue a situation that is somewhere between these two extremes will occur (Whittington et al., 2000). Such a situation is depicted in Figure 6.1 (d). Five pools of neurons have been arranged in a line to simulate a simple spatial configuration. It can be observed that inhibitory cells fire in virtually every cycle of the oscillations. In contrast, excitatory cells only fire at a subset of cycles. However, if an excitatory cell fires, is fires in synchrony with the inhibitory cells. This results in a synchronized oscillatory signal in the sum of all cells.

The abovementioned findings do not explain stimulus related resetting of ongoing oscillations. In a simulation study, Kupper et al. (2005) investigated three different mechanisms of resetting a neural network. In the first case they did not perform any resetting at all – one stimulus was simply replaced by another one. This led to increasingly scattered oscillations. In contrast, short suppression of the input between two stimuli as well as brief inhibitory pulses induced resets of the oscillations while conserving the oscillatory nature of the signal. It is well known, that brief excitatory currents can induce phase resets in Hodgkin-Huxley type neurons (e.g. Wilson, 1999, p. 152, see Tateno & Robinson, 2007 for related experimental data). Figure 6.2 illustrates a reset induced by such a brief excitatory current applied to the pyramidal cells in a PING network.

6.1.2. Cerebral systems showing γ oscillations

The data from Traub et al. (1998) and Whittington et al. (2000) are aimed to describe the emergence of γ oscillations in hippocampal and neocortical tissue. Measurements of γ oscillations have been obtained from a wide range of cortical and subcortical structures (Basar et al., 2001). Two different mechanisms for cortical (and thus potentially scalp measurable) γ oscillations have been considered. (i) The cortex itself could spontaneously generate γ oscillations (Freeman & Rogers, 2002; Singer & Gray, 1995). (ii) There could be a subcortical pacemaker (e.g. the thalamus), that drives the cortex at a frequency in the γ band which in turn leads to γ oscillations that can be measured on the scalp (Llinás et al., 1998). Thus, synchronous oscillations can also be the consequence of a common input (Whittington et al., 2000). The most important candidate for such an input signal is the thalamus. Indeed, thalamocortical connections have been associated with oscillatory activity in the γ band (Llinas et al., 2005; Steriade et al., 1996). In particular, it has been suggested that the intralaminar thalamic nuclei might drive large areas of the cortex with γ oscillations (Llinás & Ribary, 1993; Steriade et al., 1997). These nuclei constitute unspecific excitatory input to the superficial cortical layers. Furthermore, they form a PING-capable network (see Section 6.1.1) with the thalamic reticular nuclei (Steriade et al., 1997). It has been suggested, that activation of the intralaminar nuclei by sensory input relayed via the reticular formation might reset γ oscillations observed in the cortex (Körner et al., 1999).

6.2. Visual information processing with speed constraints

Different accounts have demonstrated that even complex visual tasks can be accomplished in less than 200 ms (Thorpe et al., 1996). Visual information can be utilized to guide saccade behavior after only 120 ms (Kirchner & Thorpe, 2006). Is this the normal speed of visual processing? Do we actually deal with the same type of visual processing under such "ultra-fast" response conditions? The results from Chapter 5 seem to suggest that this was not the case. Depending on temporal constraints imposed on the behavioral response, the evoked GBR is differently modulated by the perceptual task. In Section 1.2 on page 4, we introduced large scale brain oscillations as control signals for a neural timing based code. Such codes are frequently discussed in the context of feedforward processing (see Thorpe et al., 2001; VanRullen & Thorpe, 2002, for reviews). However, it is now widely agreed, that feedback plays a pivotal role in neural processing (e.g. Lamme & Roelfsema, 2000; Bar, 2004; Bullier, 2001; Sillito et al., 2006). If such a feedback signal would be manifest in sufficiently long lasting postsynaptic potentials, it could survive multiple processing frames, i.e. γ cycles, by modu-

lating the input sensitivity of specific cells (Körner et al., 1999; Crick & Koch, 1998). Such long lasting excitatory postsynaptic potentials have been described in superficial cortical layers (Cauller & Connors, 1994), where most of the cortico-cortical afferents terminate (Abeles, 1991). Such feedback could disambiguate incoming sensory information and thereby result in successive refinement of the percept (Rodemann & Körner, 2001; Körner et al., 1999).

As has been pointed out by different authors (Thorpe et al., 2001; Rolls et al., 2006), rate coding and spike latency coding are not mutually exclusive. A neuron with a higher firing rate is more likely to fire one of the first spikes of a population response. It might thus be, that only the first categorization of a stimulus is accomplished on the basis of a latency code, while later refinement processes utilize firing rate as the basic coding variable. Rolls et al. (2006) demonstrated that much of the information about a presented stimulus is already contained in the number of spikes each neuron fires in a short (20 ms) time window after response onset. Unfortunately, they only measured responses from inferior temporal cortex and did not contrast their results to a real temporal code based on synchrony or latency/phase. It is therefore not possible to infer from their data wether coding in the visual system is based on firing rates throughout the visual hierarchy, or whether the high information content carried by the firing rates is a property that emerges after the input has been distributed throughout the whole visual system (by means of either a latency or a rate code). Psychological states like perceptions, thoughts or emotions are often described as attractors of cortical dynamics (Freeman, 2003; Jirsa & Haken, 1997; Rolls et al., 1997). Although the properties and the emergence of such attractors have been described in considerable detail (Kruse et al., 1986; Freeman, 2004b,a; Rolls et al., 1997; Ohl et al., 2001), only few authors have described rapid transitions between such states (Freeman & Rogers, 2002). Interestingly Freeman & Rogers (2002) observed that spontaneous transitions between such attractors were associated with large scale, rapid, and coordinated phase slips of ongoing γ band oscillations. If such phase slips could be triggered by a stimulus, they might be measured on the scalp as evoked γ band responses.

Thus, the data presented in the current report do not conclusively support either spike based coding (Thorpe et al., 2001; Körner et al., 1999) or distributed rate coding (Rolls et al., 1997; Freeman, 2003). These two positions are, however, not mutually exclusive. While the individual neural spikes make up a distributed firing rate, it is by means of the dense interconnections between neurons, that this population firing rate determines the timing of spikes from individual neurons (e.g. Haken, 1983, S. 219). It might however be, that the information contained in the spike timings is optimal for different aspects of behaviour than is the information contained in spike rates (Fründ & Herrmann, 2007). The data presented in this report about phase-locking of evoked GBRs seem to indicate that temporal reorganization of spontaneous brain activity is crucial for linking perceptual and behavioral processing.

A. Curriculum vitae

Persönliche Angaben

Name	Ingo Fründ
Addresse	Arndtstraße 16, 39108 Magdeburg
Geburtsdatum	28. Februar 1979
Geburtsort	Schweinfurt
Familienstand	Ledig
Staatsangehörigkeit	Deutsch

Ausbildung

Seit Dez 2004	Wissenschaftlicher Mitarbeiter in der Abteilung für Biologische Psychologie am Institut für Psychologie der Otto-von-Guericke-Universität Magdeburg, in Kooperation mit dem Honda Research Institut Europa.
Okt 2002 - Nov 2004	Studium der Mathematik an der Universität Bremen
Okt 1999 - Nov 2004	Studium der Psychologie an der Universität Bremen. Diplomarbeit zum Thema: “Phasenkorrelationen im EEG gamma Band während multistabiler Wahrnehmung”.
Sep 1998 - Okt 1999	Zivildienst am “Heilpädagogischen Bildungs- und Förderzentrum”, Osnabrück
Jul 1998	Abitur am Gymnasium “In der Wüste”, Osnabrück

Praktika und Beschäftigungen während des Studiums

Mai 2001 - Nov 2004	Praktikum am Institut für Psychologie und Kognitionsforschung (Leiter Prof. Stadler) in der Gruppe von Prof. Başar-Eroğlu
Okt - Nov 2003	Praktikum am Institut für Biophysik an der Dokuz Eylül Universität, Izmir (Prof. Başar)
Sep 2003	Tutor für das mathematische Vorsemester an der Universität Bremen bei Prof. Rodenhausen und Prof. Peitgen
Feb 2003 - Jul 2003	Studentische Hilfskraft im Fachbereich Mathematik (Prof. Tretter)
Sep 2002	Tutor für das mathematische Vorsemester an der Universität Bremen bei Prof. Rodenhausen und Prof. Peitgen
Apr 2000 - Dez 2002	Studentische Hilfskraft im BLK Projekt "Lebenslanges Lernen" (Prof. Heinz)

Stipendien

Sep 2005	Stipendium des Helmholtz Insitute for Supercomputational Physics
Dec 2003 - Nov 2004	Stipendium der Studienstiftung des deutschen Volkes

Ingo Fründ

B. Danksagung

An dieser Stelle möchte ich mich bei einigen Menschen bedanken, die auf Ihre jeweilige Art und Weise zu dieser Arbeit beigetragen haben.

Christoph Herrmann hat die Arbeit betreut. Diese Betreuung war nicht nur von wissenschaftlicher Kompetenz geprägt. Darüberhinaus hat sein persönlicher Führungsstil und sein offener Umgang es leicht gemacht, nicht nur Fragen zu Phase-locking und Synchronisation, sondern auch zu türkischem Essen, dem korrekten Konsum von Hefeweizen oder seltsamen Tieren im Garten zu diskutieren. Wann sollte ich ihm sonst danken, wenn nicht an dieser Stelle.

Meinen Eltern möchte ich danken für eine gute Mischung aus kritischen Fragen und persönlicher Wertschätzung und Geborgenheit.

Lars Boenke für schöne Abende, tiefgehende Diskussionen und den Cortex Club.

Frau Körner vom Honda Research Institute Europe danke ich für die gelegentlichen anregenden Diskussionen und die Finanzierung meiner Stelle.

Weiterhin möchte ich folgenden Personen (in alphabethischer Reihenfolge) danken: Canan Başar-Eroğlu, der biologischen Psychologie in Magdeburg, dem Cortex Club, Jochen Fründ, Michael Hanke, Frank Ohl, Christiane Tretter.

In so einer Danksagung gibt es zwei prominente Orte: Den Anfang und das Ende. Darum habe ich das Ende aufgespart, um Marianne Maertens zu danken. Und die weiß, warum sie hier steht.

Literaturverzeichnis

Abeles, M. (1991). *Corticonics*. New York: Cambridge Universtity Press.

Ahissar, M. & Hochstein, S. (2004). The reverse hierarchy theory of visual perceptual learning. *TRENDS Cogn Sci*, *8*(10), 457–464.

Axmacher, N., Mormann, F., Fernandez, G., Elger, C. E., & Fell, J. (2006). Memory formation by neuronal synchronization. *Brain Res Rev*, *52*(1), 170–182.

Başar, E. (1980). *EEG-Brain Dynamics*. Amsterdam: Elsevier.

Bar, M. (2003). A Cortical Mechanism for Triggering Top-Down Facilitation in Visual Object Recognition. *J Cogn Neurosci*, *15*(4), 600–609.

Bar, M. (2004). Visual objects in context. *Nat Rev Neurosci*, *5*, 617–629.

Bar, M., Kassam, K. S., Ghuman, A. S., Boshyan, J., Schmid, A. M., Dale, A. M., Hämäläinen, M. S., Marinkovic, K., Schacter, D. L., Rosen, B. R., & Halgren, E. (2006). Top-down facilitation of visual recognition. *Proc Natl Acad Sci USA*, *103*(2), 449–454.

Basar, E. (Ed.). (1990). *Chaos in Brain Function*. Berlin: Springer.

Basar, E., Schürmann, M., Başar-Eroglu, C., & Demiralp, T. (2001). Selectively distributed gamma band system of the brain. *Int J Psychophysiol*, *39*, 129–135.

Basar-Eroglu, C., Brand, A., Hildebrandt, H., Kedzior, K. K., Mathes, B., & Schmiedt, C. (2006). Working memory related gamma oscillations in schizophrenia patients. *Int J Psychophysiol*. In Press, doi:10.1016/j.ijpsycho.2006.07.007.

Basar-Eroglu, C., Struber, D., Schurmann, M., Stadler, M., & Basar, E. (1996). Gamma-band responses in the brain: a short review of psychophysiological correlates and functional significance. *Int J Psychophysiol*, *24*(1-2), 101–112.

Berger, H. (1929). Über das Elektrenkephalogramm des Menschen. *Arch Psychiatr*, *87*, 528–570.

Brand, A., Kopmann, S., Marbach, S., Heinze, M., & Herzog, M. H. (2005). Intact and deficient feature fusion in schizophrenia. *Eur Arch Psychiatry Clin Neurosci*, *255*, 413–418.

Brown, C., Gruber, T., Boucher, J., Rippon, G., & Brock, J. (2005). Gamma abnormalities during perception of illusory figures in autism. *Cortex*, *41*(3), 364–376.

Brunia, C. H. M. (1999). Neural aspects of anticipatory behaviour. *Acta Psychologica*, *101*, 213–242.

Bullier, J. (2001). Integrated model of visual processing. *Brain Res Rev*, *36*, 96–107.

Busch, N. A., Debener, S., Kranczioch, C., Engel, A. K., & Herrmann, C. S. (2004). Size matters: effects of stimulus size, duration and eccentricity on the visual gamma-band response. *Clin Neurophysiol*, *115*(8), 1810–1820.

Busch, N. A., Herrmann, C. S., Müller, M. M., Lenz, D., & Gruber, T. (2006). A cross-laboratory study of event-related gamma activity in a standard object recognition paradigm. *NeuroImage*, *33*, 1169–1177.

Busch, N. A., Schadow, J., Fründ, I., & Herrmann, C. S. (2006). Time-frequency analysis of target detection reveals an early interface between bottom-up and top-down processes in the gamma-band. *NeuroImage*, *29*(4), 1106–1116.

Cariani, P. A. (2004). Temporal Codes and Computations for Sensory Representation and Scene Analysis. *IEEE Transactions on Neural Networks*, *15*(5), 1100–1111.

Cauller, L. J. & Connors, B. W. (1994). Synaptic physiology of horizontal afferents to layer I in slices of rat SI neocortex. *J Neurosci*, *14*(2), 751–762.

Chatrian, G. E., Lettich, E., & Nelson, P. L. (1985). Ten percent electrode system for topographic studies of spontaneous and evoked eeg activity. *Am J EEG Technol*, *25*, 83–92.

Chen, A. C. & Herrmann, C. S. (2001). Perception of pain coincides with the spatial expansion of electroencephalographic dynamics in human subjects. *Neurosci Lett*, *297*(3), 183–186.

Crick, F. & Koch, C. (1998). Constraints on cortical and thalamic projections: the no-strong-loops hypothesis. *Nature*, *391*, 245–250.

Dayan, P. & Abbott, L. F. (2001). *Theoretical Neuroscience*. Cambridge: MIT Press.

De Pascalis, V. & Ray, W. J. (1998). Effects of memory load on event-related patterns of 40-Hz eeg during cognitive and motor tasks. *Int J Psychophysiol*, *28*, 301–315.

Debener, S. & Engel, A. K. (2005). Kommentar zu C. S. Herrmann: Gamma-Aktivität. Die psychopathologische Bedeutung hochfrequenter EEG-Oszillationen. *Zeitschrift für Neuropsychologie*, *16*(3).

Debener, S., Herrmann, C. S., Kranczioch, C., Gembris, D., & Engel, A. K. (2003). Top-down attentional processing enhances auditory evoked gamma band activity. *NeuroReport*, *14*(5), 683–686.

Debener, S., Kranczioch, C., Herrmann, C., & Engel, A. (2002). Auditory novelty oddball allows reliable distinction of top-down and bottom-up processes of attention. *Int J Psychophysiol*, *46*(1), 77–84.

Deecke, L., Bashore, T., Brunia, C. H., Grunewald-Zuberbier, E., Grunewald, G., & Kristeva, R. (1984). Movement-associated potentials and motor control. Report of the EPIC IV Motor Panel. *Annals of the New York Academy of Sciences*.

Destexhe, A., Rudolph, M., & Paré, D. (2003). The high-conductance state of neocortical neurons in vivo. *Nat Rev Neurosci*, *4*, 739–751.

Endl, W., Wall, P., Lindinger, G., Deecke, L., & Lang, W. (1999). Event-related potential correlate of false recognition of faces. *Neuroscience Letters*, *265*, 115–118.

Endo, H., Kizuka, T., Masuda, T., & Takeda, T. (1999). Automatic aciviation in the human primary motor cortex synchronized with movement preparation. *Cognitive Brain Research*, *3*, 229–239.

Engel, A. K., Fries, P., & Singer, W. (2001). Dynamic predictions: Oscillations and synchrony in top-down processing. *Nat Rev Neurosci*, *2*, 704–716.

Fell, J., Fernández, G., Klaver, P., Egler, C. E., & Fries, P. (2003). Is synchronized neuronal gamma activity relevant for selective attention? *Brain Res Rev*, *42*, 265–272.

Fell, J., Köhling, R., Grunwald, T., Klaver, P., Dietl, T., Schaller, C., Becker, A., Egler, C. E., & Fernández, G. (2005). Phase-locking characteristics of limbic P3 responses in hippocampal sclerosis. *NeuroImage*, *24*, 980–989.

Fisher, N. (1993). *Statistical analysis of circular data*. New York: Cambridge Universtity Press.

Freeman, W. J. (1975). *Mass Action in the Nervous System*. New York: Academic Press.

Freeman, W. J. (2003). The wave packet: an action potential for the 21st century. *J Integrat Neurosci*, *2*(1), 3–30.

Freeman, W. J. (2004a). Origin, structure, and role of background EEG activity. Part 1. Analytic amplitude. *Clin Neurophysiol*, *115*, 2077–2088.

Freeman, W. J. (2004b). Origin, structure, and role of background EEG activity. part 2. analytic phase. *Clin Neurophysiol*, *115*, 2089–2107.

Freeman, W. J. & Rogers, L. J. (2002). Fine temporal resolution of analytic phase reveals episodic synchronization by state transitions in gamma EEGs. *J Neurophysiol*, *87*, 937–945.

Fregnac, Y., Monier, C., Chavane, F., Baudot, P., & Graham, L. (2003). Shunting inhibition, a silent step in visual cortical computation. *J Physiol (Paris)*, *97*, 441–451.

Freude, G., Ullsperger, P., Kruger, H., & Pietschmann, M. (1989). Bereitschaftspotential and the efficiency of mental task performance. *J Psychophysiol*, *3*(4), 377–385.

Fries, P., Neuenschwander, S., Engel, A. K., Goebel, R., & Singer, W. (2001). Rapid feature selective neuronal synchronization through correlated latency shifting. *Nat Neurosci*, *4*(2), 194–200.

Fründ, I., Busch, N. A., Körner, U., Schadow, J., & Herrmann, C. S. (2007). EEG oscillations in the gamma and alpha range respond differently to spatial frequency. *Vision Res*, *47*(15), 2086–2098.

Fründ, I. Busch, N. A., Schadow, J., Gruber, T., Körner, U. & Herrmann, C. S. (2007). Time pressure modulates electrophysiological correlates of early visual processing. *PLoS one*, *3*(2), e1675.

Fründ, I., Busch, N. A., Schadow, J., Körner, U., & Herrmann, C. S. (2007). From perception to action: phase-locked gamma oscillations correlate with reaction times in a speeded response task. *BMC Neurosci*, *8*(27).

Fründ, I. & Herrmann, C. S. (2007). Simulating evoked gamma oscillations of human eeg in a network of spiking neurons reveals an early mechanism of memory matching. *AIP Proc*, *913*.

Fründ, I., Schadow, J., Busch, N. A., Körner, U., & Herrmann, C. S. (2007). Evoked gamma oscillations in human scalp EEG are test-retest reliable. *Clin Neurophysiol*, *118*(1), 221–227.

Funke, K. & Wörgötter, F. (1997). On the significance of temporally structured activity in the dorsal lateral geniculate nucleaus (LGN). *Prog Neurobiol*, *53*, 67–119.

Grey Walter, W. (1964). Contingent negative variation: An electrical sign of sensorimotor association and expectancy in the human brain. *nature*, *203*, 380–384.

Grice, S. J., Spratling, M. W., Karmiloff-Smith, A., Halit, H., Csibra, G., de Haan, M., & Johnson, M. H. (2001). Disordered visual processing and oscillatory brain activity in autism and Williams Syndrome. *Neuro Report*, *12*(12), 2697–2700.

Gruber, T. & Müller, M. M. (2005). Oscillatory brain activity dissociates between associative stimulus content in a repetition priming task in the human EEG. *Cereb Cortex*, *15*(1), 109–116.

Gruber, T. & Müller, M. M. (2006). Oscillatory brain activity in the human EEG during indirect and direct memory tasks. *Brain Res*, *1097*(1), 194–204.

Haig, A. R., De Pascalis, V., & Gordon, E. (1999). Peak gamma latency correlated with reaction time in a conventional oddball paradigm. *Clinical Neurophysiology*, *110*, 158–165.

Haken, H. (1983). *Synergetik* (2nd ed.). Berlin: Springer.

Herrmann, C. S. & Demiralp, T. (2005). Human EEG gamma oscillations in neuropsychiatric disorders. *Clin Neurophysiol*, *116*, 2719–2733.

Herrmann, C. S., Grigutsch, M., & Busch, N. A. (2005). EEG oscillations and wavelet analysis. In T. C. Handy (Ed.), *Event-Related Potentials - A Methods Handbook* (pp. 229–259). MIT Press.

Herrmann, C. S., Lenz, D., Junge, S., Busch, N. A., & Maess, B. (2004). Memory-matches evoke human gamma-responses. *BMC Neurosci*, *5*(13).

Herrmann, C. S. & Mecklinger, A. (2000). Magnetoencephalographic responses to illusory figures: early evoked gamma is affected by processing of stimulus features. *Int J Psychophysiol*, *38*(3), 265–281.

Herrmann, C. S., Mecklinger, A., & Pfeifer, E. (1999). Gamma responses and ERPs in a visual classification task. *Clin Neurophysiol*, *110*(4), 636–642.

Herrmann, C. S., Munk, M. H., & Engel, A. K. (2004). Cognitive functions of gamma-band activity: memory match and utilization. *TRENDS Cogn Sci*, *8*(8), 347–355.

Hochstein, S. & Ahissar, M. (2002). View from the top: Hierarchies and reverse hierarchies in the visual System. *Neuron*, *36*(5), 791–804.

Hoogenboom, N., Schoffelen, J.-M., Oostenveld, R., Parkes, L. M., & Fries, P. (2006). Localizing human visual gamma-band activity in frequency, time and space. *NeuroImage*, *29*(3), 764–773.

Hopfield, J. J. (1995). Pattern recognition computation using action potential timing for stimulus representation. *Nature*, *376*, 33–36.

Izhikevich, E. M. (2003). Simple model of spiking neurons. *IEEE Trans Neural Networks*, *14*(6), 1569–1572.

Jacobs, J., Kahana, M. J., Ekstrom, A. D., & Fried, I. (2007). Brain oscillations control timing of single-neuron activity in humans. *J Neurosci*, *27*(14), 3839–3844.

Jasper, H. H. (1958). The ten-twenty electrode system of the international federation. *Electroencephalogr Clin Neurophysiol*, *10*, 371–375.

Jensen, O., Gelfand, J., Kounios, J., & Lisman, J. E. (2002). Ocillations in the alpha band (9-12 Hz) increase with memory load during retention in a short-term memory task. *Cereb Cortex*, *12*, 877–882.

Jirsa, V. K. & Haken, H. (1997). A derivation of a macroscopic field theory of the brain from the quasi-microscopic neural dynamics. *Physica D*, *99*, 503–526.

Jokeit, H. (1990). Analysis of periodicities in human reaction times. *Naturwissenschaften*, *77*, 289–291.

Jokeit, H. & Makeig, S. (1994). Different event-related patterns of gamma-band power in brain waves of fast- and slow-reacting subjects. *Proc Natl Acad Sci, USA*, *91*(14), 6339–6343.

Kaiser, J. & Lutzenberger, W. (2005). Human gamma-band activity: A window to cognitive processing. *NeuroReport*, *16*(3), 207–211.

Karakaş, S. & Başar, E. (1998). Early gamma response is sensory in origin: a conclusion based on cross-comparison of results from multiple experimental paradigms. *Int J Psychophysiol*, *31*, 13–31.

Kazantsev, V. B., Nekorkin, V. I., Makarenko, V. I., & Llinás, R. (2004). Self-referential phase reset based on inferior olive oscillator dynamics. *Proc Natl Acad Sci, USA*, *101*(52), 18183–18188.

Keil, A., Gruber, T., & Müller, M. M. (2001). Functional correlates of macroscopic high-frequency brain activity in the human visual system. *Neurosci Biobehav Rev*, *25*, 527–534.

Keil, A., Stolarova, M., Heim, S., Gruber, T., & Müller, M. M. (2003). Temporal stability of high-frequency brain oscillations in the human EEG. *Brain Topogr*, *16*(2), 101–110.

Kirchner, H. & Thorpe, S. J. (2006). Ultra-rapid object detection with saccadic eye movements: Visual processing speed revisited. *Vision Res*, *46*, 1762–1776.

Klimesch, W. (1999). EEG alpha and theta oscillations reflect cogni tive and memory performance: a review and analysis. *Brain Res Brain Res Rev*, *29*(2-3), 169–195.

Klimesch, W., Hanslmayr, S., Sauseng, P., Gruber, W., Brozinsky, C. J., Kroll, N. E. A., Yonelinas, A. P., & Doppelmayr, M. (2006). Oscillatory EEG Correlates of Episodic Trace Decay. *Cereb Cortex*, *16*(2), 280–290.

König, P. & Krüger, N. (2006). Symbols as self-emergent entities in an optimization process of feature extraction and predictions. *Biol Cybern*, *94*, 325–334.

Körding, K. P. & König, P. (2000). A learning rule for dynamic recruitment and decorrelation. *Neural Networks*, *13*, 1–9.

Körner, E., Gewaltig, M.-O., Körner, U., Richter, A., & Rodemann, T. (1999). A model of computation in neocortical architecture. *Neural Networks*, *12*, 989–1005.

Kruse, P., Stadler, M., & Wehner, T. (1986). Direction and frequency specific processing in the perception if long-range apparent movement. *Vision Res*, *26*(2), 327–335.

Kupper, R., Gewaltig, M.-O., Körner, U., & Körner, E. (2005). Spike-latency codes and the effect of saccades. *Neurocomputing*, *65–66*, 189–194.

Lachaux, J.-P., George, N., Tallon-Baudry, C., Martinerie, J., Hugueville, L., Minotti, L., Kahane, P., & Renault, B. (2005). The many faces of the gamma band response to complex visual stimuli. *NeuroImage*, *25*, 491–501.

Lamme, V. A. F. & Roelfsema, P. R. (2000). The distinct modes of vision offered by feedforward and recurrent processing. *TRENDS in Neurosci*, *23*(11), 571–579.

Lee, K. H., Williams, L. M., Breakspeak, M., & Gordon, E. (2003). Synchronous gamma activity: a review and contribution to an integrative neuroscience model of schizophrenia. *Brain Res Brain Res Rev*, *41*(1), 57–78.

Lee, K.-H., Williams, L. M., Haig, A., Goldberg, E., & Gordon, E. (2001). An integration of 40 Hz gamma and phasic arousal: novelty and routinization processing in schizophrenia. *Clin Neurophysiol*, *112*, 1499–1507.

Lengyel, M., Huhn, Z., & Érdí, P. (2005). Computational theories on the function of theta oscillations. *Biol Cybern*, *92*, 393–408.

Leocani, L., Toro, C., Zhuang, P., Gerloff, C., & Hallet, M. (2001). Event-related desynchronization in reaction time paradigms: a comparison with event-related potentials and corticospinal excitability. *Clin Neurophysiol*, *112*, 923–930.

Llinás, R. & Ribary, U. (1993). Coherent 40-Hz oscillation characterizes dream state in humans. *Proc Natl Acad Sci, USA*, *90*, 2078–2081.

Llinás, R., Ribary, U., Contreras, D., & Pedroarena, C. (1998). The neuronal basis for consciousness. *Phil Trans R Soc Lond*, *353*, 1841–1849.

Llinas, R., Urbano, F. J., Leznik, E., Ramirez, R. R., & van Marle, H. J. F. (2005). Rhythmic and dysrhythmic thalamocortical dynamics: GABA systems and the edge effect. *TRENDS in Neurosci*, *28*(6), 325–333.

Louis, A. K., Maaß, P., & Rieder, A. (1998). *Wavelets* (2 ed.). Wiesbaden, Germany: Teubner.

Makarenko, V. & Llinás, R. (1998). Experimentally determined chaotic phase synchronization in a neuronal system. *Proc Natl Acad Sci, USA*, *95*, 15747–15752.

Makeig, S., Westerfield, M., Jung, T.-P., Enghoff, S., Townsend, J., Courchesne, E., & Sejnowski, T. J. (2002). Dynamic brain sources of visual evoked responses. *science*, *295*, 690–694.

Morup, M., Hansen, L. K., Herrmann, C. S., Parnas, J., & Arnfred, S. M. (2006). Parallel factor analysis as an exploratory tool for wavelet transformed event-related EEG. *NeuroImage*, *29*(3), 938–947.

Moss, F., Ward, L. M., & Sannita, W. G. (2004). Stochastic resonance and sensory information processing: a tutorial and review of application. *Clin Neurophysiol*, *115*, 267–281.

Neuper, C. & Pfurtscheller, G. (2001). Event-related dynamics of cortical rhythms: frequency-specific features and functional correlates. *Int J Psychophysiol*, *43*, 41–58.

Nolte, G., Bai, O., Wheaton, L., Mari, Z., Vorbach, S., & Hallett, M. (2004). Identifying true brain interaction from eeg data using the imaginary part of coherency. *Clin Neurophysiol*, *115*(10), 2292–2307.

Nunez, P. L. & Srinivasan, R. (2006). *Electric Fields of the Brain* (2nd ed.). New York: Oxford University Press.

Ohl, F. W., Scheich, H., & Freeman, W. J. (2001). Change in pattern of ongoing cortical activity with auditory category learning. *Nature*, *412*(6848), 693–694.

Olufsen, M. S., Whittington, M. A., Camperi, M., & Kopell, N. (2003). New roles for the gamma rhythm: Population tuning and preprocessing for the beta rhythm. *J Comput Neurosci*, *14*(1), 33–54.

Oppenheim, A. V., Schafer, R. W., & Buck, J. R. (2004). *Zeitdiskrete Signalverarbeitung* (2nd revised ed.). Pearson.

Pineda, J. A. (2005). The functional significance of mu rhythms: translating "seeing" and "hearing" into "doing". *Brain Res Rev*, *50*, 57–68.

Plainis, S. & Murray, I. J. (2000). Neurophysiological interpretation of human visual reaction times: effect of contrast, spatial frequency and luminance. *Neuropsychologia*, *38*(2), 1555–1564.

R Development Core Team (2004). *R: A language and environment for statistical computing*. Vienna, Austria: R Foundation for Statistical Computing. 3-900051-07-0.

Ribary, U., Ioannides, A. A., Singh, K. D., Hasson, R., Bolton, J. P. R., Lado, F., Mogilner, A., & Llinás, R. (1991). Magetic field tomography of coherent thalamocortical 40-Hz oscillations in humans. *Proc Natl Acad Sci, USA*, *88*, 11037–11041.

Rodemann, T. & Körner, E. (2001). Two separate processing streams in a cortical-type architecture. *Neurocomputing*, *38–40*, 1541–1547.

Rodemann, T. & Körner, E. (2003). Information processing with spiking neurons in a cortical architecture framework under the control of an oscillatory signal. *Neurocomputing*, *52–54*, 901–906.

Rodriguez, E., George, N., Lachaux, J.-P., Martinerie, J., Renault, B., & Varela, F. J. (1999). Perception's shadow: long distance synchronization of human brain activity. *nature*, *397*, 430–433.

Roelfsema, P. R., Engel, A. K., König, P., & Singer, W. (1997). Visuomotor integration is associated with zero time-lag synchronization amoung cortical areas. *Nature*, *385*(6612), 157–161.

Rolls, E. T., Franco, L., Aggelopoulos, N. C., & Jerez, J. M. (2006). Information in the first spike, the order of spikes, and the number of spikes provided by neurons in the inferior temporal visual cortex. *Vision Res*, *46*(25), 4193–4205.

Rolls, E. T., Treves, A., & Tovee, M. J. (1997). The representational capacity of the distributed encoding of information provided by populations of neurons in primate temporal visual cortex. *Exp Brain Res*, *114*(1), 149–162.

Rossion, B. & Pourtois, G. (2004). Revisiting Snodgrass and Vanderwart's object pictorial set: The role of surface detail in basic-level object recognition. *Perception*, *33*, 217–236.

Rosso, O. A., Blanco, S., Yordanova, J., Kolev, V., Figliola, A., Schurmann, M., & Basar, E. (2001). Wavelet entropy: a new tool for analysis of short duration brain electrical signals. *J Neurosci Methods*, *105*(1), 65–75.

Sarbadhikari, S. N. & Chakrabarty, K. (2001). Chaos in the brain: a short review alluding to epilepsy, depression, exercise and lateralization. *Med Eng Phys*, *23*(7), 445–455.

Schechter, I., Butler, P. D., Zemon, V. M., Revheim, N., Saperstein, A. M., Jalbrzikowsi, M., Pasternak, R., Silipo, G., & Javitt, D. C. (2005). Impairments in generation of early-stage transient visual evoked potentials to magno- and parvocellular-selective stimuli in schizophrenia. *Clin Neurophysiol*, *116*, 2204–2215.

Schmiedt, C., Brand, A., Hildebrandt, H., & Basar-Eroglu, C. (2005). Event-related theta oscillations during working memory tasks in patients with schizophrenia and healthy controls. *Cognitive Brain Research*, *25*, 936–947.

Sergi, M. J. & Green, M. F. (2002). Social perception and early visual processing in schizoprenia. *Schizophrenia Research*, *59*, 233–241.

Sewards, T. V. & Sewards, M. A. (1999). Alpha-band oscillations in visual cortex: part of the neural correlate of visual awareness? *Int J Psychophysiol*, *32*, 35–45.

Sillito, A. M., Cudeiro, J., & Jones, H. E. (2006). Always returning: feedback and sensory processing in visual cortex and thalamus. *TRENDS in Neurosci*, *29*(6), 307–316.

Singer, W. & Gray, C. M. (1995). Visual feature integration and the temporal correlation hypothesis. *Annu Rev Neurosci*, *18*, 555–586.

Spencer, K. M., Nestor, P. G., Niznikiewicz, M. A., Salisbury, D. F., Shenton, M. E., & McCarley, R. W. (2003). Abnormal neural synchrony in schizophrenia. *J Neurosci*, *23*(19), 7407–7411.

Spencer, K. M., Nestor, P. G., Perlmutter, R., Niznikiewicz, M. A., Klump, M. C., Frumin, M., Shenton, M. E., & McCarley, R. W. (2004). Neural synchrony indexes disordered perception and cognition in schizophrenia. *Proc Natl Acad Sci, USA*, *101*(49), 17288–17293.

Stam, C. J. (2005). Nonlinear dynamical analysis of EEG and MEG: review of an emerging field. *Clin Neurophysiol*, *116*(10), 2266–2301.

Steriade, M., Contreras, D., Amzica, F., & Timofeev, I. (1996). Synchronization of fast (30-40 Hz) spontaneous oscillations in intrathalamic and thalamocortical networks. *J Neurosci*, *16*(8), 2788–2808.

Steriade, M., Jones, E. G., & McCormick, D. A. (1997). *Thalamus*, volume 1. Amsterdam: Elevier.

Tallon-Baudry, C. & Bertrand, O. (1999). Oscillatory gamma activity in humans and its role in object representation. *TRENDS Cogn Sci*, *3*(4), 151–162.

Tallon-Baudry, C., Bertrand, O., Delpuech, C., & Pernier, J. (1996a). Stimulus specificity of phase-locked and non-phase-locked 40 Hz visual responses in human. *J Neurosci*, *16*(13), 4240–4249.

Tallon-Baudry, C., Bertrand, O., Delpuech, C., & Pernier, J. (1996b). Stimulus specificity of phase-locked and on-phase-locked 40 Hz visual responses in human. *J Neurosci*, *16*(13), 4240–4249.

Tallon-Baudry, C., Bertrand, O., Delpuech, C., & Pernier, J. (1997). Oscillatory γ-band (30-70 hz) activity induced by a visual search task in humans. *J Neurosci*, *17*(2), 722–734.

Tallon-Baudry, C., Bertrand, O., Peronnet, F., & Pernier, J. (1998). Induced γ-band activity during the delay of a visual short-term memory task in humans. *J Neurosci*, *18*(11), 4244–4254.

Talsma, D. & Woldorff, M. G. (2005). Methods for the Estimation and Removal of Artifacts and Overlap in ERP Waveforms. In Handy, T. (Ed.), *Event-related potentials. A methods Handbook*, (pp. 115–148)., Cambridge, Massachusetts. MIT Press.

Tateno, T. & Robinson, H. P. C. (2007). Phase resetting curves and oscillatory stability in interneurons of rat somatosensory cortex. *Biophys J*, *92*, 683–695.

Thielscher, A. & Neumann, H. (2006). Neural mechanisms of cortico-cortical interaction in texture boundary detection: a modeling approach. *Neuroscience*, *122*, 921–939.

Thorpe, S., Delorme, A., & Van Rullen, R. (2001). Spike-based strategies for rapid processing. *Neural Networks*, *6-7*(14), 715–725.

Thorpe, S., Fize, D., & Marlot, C. (1996). Speed of processing in the human visual system. *Nature*, *381*(6582), 520–522.

Tiitinen, H., Sinkkonen, J., Reinikainen, K., Alho, K., Lavikainen, J., & Näätänen, R. (1993). Selective attention enhances the auditory 40-Hz transient response in humans. *Nature*, *364*, 59–60.

Traub, R. D., Spruston, N., Soltesz, I., Konnertz, A., Whittington, M. A., & Jefferys, J. G. R. (1998). Gamma-frequency oscillations: a neuronal population phenomenon, regulated by synaptic and intrinsic cellular processes, and inducing synaptic plasticity. *Prog Neurobiol*, *55*, 563–575.

Trillenberg, P., Verleger, R., Wascher, E., Wauschkuhn, B., & Wessel, K. (2000). CNV and temporal uncertainty with 'ageing' and 'non-ageing' S1-S2 intervals. *Clin Neurophysiol*, *111*(7), 1216–1226.

VanRullen, R. & Koch, C. (2003). Is perception discrete or continuous? *TRENDS Cogn Sci*, *7*(5), 207–213.

VanRullen, R. & Thorpe, S. J. (2002). Surfing a spike wave down the ventral stream. *Vision Res*, *42*, 2593–2615.

Vorberg, D. & Schwarz, W. (1987). Oscillatory mechanisms in human reaction times? *Naturwissenschaften*, *74*, 446–447.

Wehr, M. & Zador, A. M. (2003). Balanced inhibition underlies tuning and sharpens spike timing in auditory cortex. *Nature*, *426*, 442–446.

Whittington, M. A., Traub, R. D., Kopell, N., Ermentrout, B., & Buhl, E. H. (2000). Inhibition-based rhythms: experimental and mathematical observations on network dynamics. *Int J Psychophysiol*, *38*, 315–336.

Wilson, H. R. (1999). *Spikes, decisions and actions. Dynamical foundations of neuroscience*. New York: Oxford University Press.

Wright, J. J., Sergejew, A. A., & Stampfer, H. G. (1990). Inverse filter computation of the neural impulse giving rise to the auditory evoked potential. *Brain Topography*, *2*(4), 293–302.

Wyss, R., König, P., & Verschure, P. F. M. J. (2003). Invariant representations of visual patterns in a temporal population code. *Proc Natl Acad Sci, USA*, *100*(1), 324–329.

Yordanova, J., Banaschewski, T., Kolev, V., Woerner, W., & Rothenberger, A. (2001). Abnormal early stages of task stimulus processing in children with attention-deficit hyperactivity disorder–evidence from event-related gamma oscillations. *Clin Neurophysiol*, *112*(6), 1096–1108.

Yordanova, J., Kolev, V., & Demiralp, T. (1997). The phase-locking of auditory gamma band responses in humans is sensitive to task processing. *NeuroReport*, *8*, 3999–4004.